

**The preparation of an immunosensor for the detection of
microcystins and nodularins by immobilisation of a labelled
antibody onto a polymer modified electrode**

Robert Matthew Siebritz



A thesis submitted in fulfilment of the requirements for the completion of Masters
Project in the Department of Chemistry, University of Western Cape.

Supervisor: Prof. P. Baker and Prof E. Iwuoha

NOVEMBER 2011

**The preparation of an immunosensor for the detection of
microcystins and nodularins by immobilisation of a labelled
antibody onto a polymer modified electrode**

Robert Matthew Siebritz

KEYWORDS

Microcystin & Nodularins

ELISA

Immunosensor

ADDA,

Cyanobacteria,

Blue-green algae,

Anti-sheep IgG antibody,

Antigen

Potable water

Cyclic voltammetry



ABSTRACT

South African dams and reservoirs are increasingly showing the propensity to support sustained populations of Cyanobacteria (blue green algae). These photosynthetic bacteria occur throughout the world and can rapidly form blooms in eutrophic water systems.

The occurrence of these photosynthetic bacteria, in our dwindling drinking water source dams, poses a serious, economic, as well as a health, threat to an arid country like South Africa due to its potential to produce toxic metabolites like Microcystins and Nodularins (MCN). MCN's are cyclic peptide toxins, harmful to humans and animals, and its toxicological mechanism is based on a strong inhibition of protein phosphatases in the liver. This may lead to severe liver damage and increased tumour development. Rural communities consuming untreated water in South Africa are most at risk due to the high toxicity of MCN's at low doses.

We endeavour to develop an immunosensor for the detection of Microcystins and nodularins using anti-sheep IgG antibody labelled with horseradish peroxidase (HRP) immobilised on a modified glassy-carbon polymer surface. The immunosensor will be applied to water samples for MCN's as a group of compounds recognised by the ADDA moiety common to all MCN congeners. The immunosensor will provide immediate confirmation and quantification of MCN's in situ.

A competitive Enzyme Linked Immuno-Sorbant Assay (ELISA) and High Performance liquid Chromatography (HPLC) will be used to validate results of our immunosensor. Elisa's are widely used as a screening test method for MCN's. The antibody-antigen specificity forms the bases for the recognition of target compound (MCN's) by antibodies which bind to a compound which is labelled with a colour indicator, and quantified by spectrophotometry.

Key Words: Microcystin, Nodularins, Elisa, Immunosensor, HPLC, horseradish peroxidase (HRP), ADDA, Cyanobacteria, blue-green algae, ant-sheep IgG antibody,



DECLARATION

I declare that *The preparation of an immunosensor for the detection of microcystins and nodularins by immobilisation of a labelled antibody onto a polymer modified electrode* is my own work, that it has not been submitted before for any degree or examination in any other university, and that all the sources I have used or quoted have been indicated or acknowledged as complete references.



Robert Matthew Siebritz

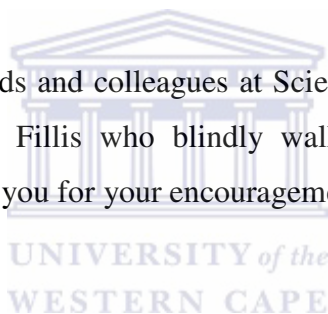
November 2011

Signed _____

ACKNOWLEDGEMENTS

Firstly, I will like to give the God Almighty all the glory, honour and adoration for seeing me through this great journey. The personal trials that made this journey seem almost impossible was it not for His presence, it has really been an interesting and fulfilling venture. To my supervisors, Dr. Priscilla Baker and Professor Emmanuel Iwuoha, I say a big thank you for your untiring efforts and interest in this work. In particular Prof Baker, that has been extremely patient and caring of the part-time students. Your confidence in me was indeed a great inspiration. To the staff and members of the Sensor Laboratory, I say a big thank you for the amicable working environment you created during my studies. You were always willing to assist. To the National Research Foundation (NRF) of South Africa, thank you for awarding me a bursary.

I wish to thank my friends and colleagues at Scientific Services especially Heidi Richards and Ismeralda Fillis who blindly walk with me into the world of Electrochemistry. Thank you for your encouragement.



Finally, to all my family members, I say thank you. I am particularly grateful to my parents, for taking care of my children and wife and garden in my absence, thank you for my education and upbringing. To my siblings, Ruth and Timmy thank you for keeping my family together when I was not around.

To my dear wife, Colette, and my children, Matthew and Leah, I would like to thank you for your patience and understanding, for taking care of the household when I was at work or studying. I appreciated all the little things you did notes of encouragement to unexpected cups of tea. I am forever grateful for your kind and loving support.

LIST OF ABBREVIATIONS

AB	Antibody for Microcystins and Nodularins raised in sheep.
ADDA	unusual amino acid, unique to cyanobacterial toxins: (2S, 2S, 8S, 9S)-3-amino-9-methoxy-2,6,8-trimethyl-10-phenyldeca-4,6-dienoic acid
AG1, AG2, AG3	Antigen from ELISA kit with numerical value indicating the number of the serial addition
DPV	Differential Pulse Voltammetry
DWA	Department of Water Affairs
EIS	Electrochemical Impedance Spectroscopy
ELISA	Enzyme Linked Immuno-Sorbant Assay
GCE	Glassy Carbon Electrode
GCE/PPY	Polypyrrole modified Glassy carbon Electrode
GCE/PPY/AB	Polypyrrole modified Glassy carbon Electrode with drop-coated Antibody = immunosensor
HPLC	High Performance Liquid Chromatography
IgG	Immunoglobulin Antibody
MCN	Microcystins and Nodularin
MYC	Microcystin-LR equivalents
OSWV	Osteryoung Square wave voltammetry
OX	Refers to Anodic or oxidative measurements peaks
PPIA	Protein Phosphatase Inhibition Assays
RED	Refers to cathodic or reductive measurements/peaks
SMP	Refers to Real sample
WHO	World Health Organization

LIST OF FIGURES AND TABLES

FIGURES

- Figure 1 Microcystin-LR, where Z – Arginine and X - Leucine
- Figure 2 Structure of Nodularin
- Figure 3 Abraxis ELISA standard curves showing good agreement between variants of Microcystins and Nodularins
- Figure 4 HPLC and Extraction unit used to concentrate toxins in raw water samples
- Figure 5 ELISA reader, Kit contents and Microwell Plates
- Figure 6 Schematic Representation of the ADDA Indirect Competitive ELISA
- Figure 7 Abraxis ADDA ELISA kit
- Figure 8 Time series showing trends of ELISA toxin data at Voëlvele Water Treatment Works
- Figure 9 Typical cyclic voltammogram showing reduction and oxidation peaks
- Figure 10 Typical Bode Plot (a) and Typical Nyquist Plot (b)
- Figure 11 Randles equivalent circuit for a simple electrochemical cell
- Figure 12 Cyclic Voltammogram of the polymerization of Polypyrrole in 0.1 M HCl over the potential window of -400 to 700 mV at a scan rate of 50 mV/s for 10 cycles on a GCE electrode.
- Figure 13 Characterization GCE/PPy electrode at different scan rates (a=5, b=10, c= 20, d= 50 & e= 100 mV/s) using cyclic voltammetry
- Figure 14 Plot of Square root of scan rate vs Current (A) for GCE/PPY film in 0.1 M HCl.
- Figure 15 Characterization of GCE/PPY in 0.1 M PBS (pH 7.0) at scan rates (a=5, b=10, c= 20, d= 50 & e= 100 mV/s)
- Figure 16 Plot of Square root of scan rate vs Current (I_{pa}) of for GC/PPY in PBS 0.1M PBS (pH7.0)
- Figure 17 The multi –scan rate cyclic voltammograms for the Immunosensor (GCE/PPY/AB) (a= 10, b =20, c=50 and d = 100 mV/s)
- Figure 18 Figure 18. Multi-scan rate using OSWV of the immunosensor (GCE/PPy/AB) for the Anodic sweep

Figure 19	Figure 19. Multi-scan rate using OSWV of the immunosensor (GCE/PPy/AB) for the Cathodic sweep
Figure 20	Multi-scan rate using DPV of the immunosensor (GCE/PPy/AB) for the anodic sweep
Figure 21	Multi-scan rate using DPV of the immunosensor (GCE/PPy/AB) for the cathodic sweep
Figure 22	Oxidative (a) and reductive (b) OSWV for immunosensor response to increasing Antigen concentration
Figure 23	Oxidative (left) and reductive (Right) DPV for immunosensor response to increasing Antigen concentration and a scan rate of 50 mV/s
Figure 24	Calibration curve using anodic OSWV peak response.
Figure 25	Calibration curve using cathodic SWV peak response
Figure 26	Calibration curve using anodic DPV peak response
Figure 27	Calibration curve using cathodic DPV peak response
Figure 28	OSWV of immunosensor (GCE/PPY/AB) anodic response to real samples from Voëlvlei Dam
Figure 29	OSWV of immunosensor (GCE/PPY/AB) anodic response to real samples from Voëlvlei dam

TABLES

Table 1	The effects of Microcystin on Human Health
Table 2	Comparison of HPLC and ELISA methods for Toxin Analysis
Table 3	Measuring Principles for ELISA Types (from Biosense)
Table 4	ELISA summary results for Faure and Voëlvlei waters
Table 5	Average peak potentials calculated for different scan rates for the anodic and cathodic observed
Table 6	Average peak potentials calculated for different scan rates for the anodic and cathodic observed

Table 7	Calibration curve data for OSWV
Table 8	Calibration curve data for DPV
Table 9	Showing the Peak currents and difference in peak currents of sample and immunosensor using OSWV
Table 10	Showing the Peak currents and difference in peak currents of sample and immunosensor using DPV
Table 11	Comparison of results from ELISA and Immunosensor

Contents

Title Page	1
Keywords	2
Abstract	3
Declaration	5
Acknowledgements	6
List of Abbreviations	7
List of Figures & Tables	8
Table of contents	10



TABLE OF CONTENTS

Chapter 1.....	13
1.1 Introduction.....	13
1.2 Harmful algal blooms.....	14
1.3 Cyanobacteria – Toxins.....	15
1.4 The chemical structure of Microcystins.....	16
1.5 Toxicity of Microcystins & Nodularins (MCN's) and their Health Impacts.....	18
1.6 Detection Methods for Monitoring of Microcystins & Nodularins.....	20
1.7 Human Risk to chronic exposure.....	24
Chapter 2.....	26
2.1 Introduction:.....	26
2.2 Algal Monitoring in the City of Cape Town.....	27
2.3 Enzyme-Linked Immuno-Sorbent Assays.....	30
2.4 An ADDA Elisa kit is available from Abraxis.....	33
2.5 Findings of ELISA data collected from raw water, Cape Town.....	35
Chapter 3.....	40
Methodology.....	40
3.1 Electrochemistry.....	40
3.1.1 Cyclic voltammetry.....	42
3.1.2 Square wave voltammetry.....	43
3.1.3 Differential Pulse Voltammetry.....	44
3.2 Electrochemical Impedance Spectroscopy (EIS).....	46
3.2.1 Background.....	46
3.2.2 Nyquist & Bode Plots.....	48
3.3 Reagents and instrumentation.....	51
3.3.1 Reagents.....	51

3.3.2 Instrumentation	51
Chapter 4	53
Results and discussion	53
4.1 Instrumentation :	53
4.2 Synthesis of Polypyrrole.....	54
4.3 Characterization of Polypyrrole Modified Glassy Carbon electrode (GCE)	56
4.4 Preparation of Immunosensor	59
4.5 Cyclic Voltammetry.....	60
4.5.1 Cyclic Voltammetric Investigation of Immunosensor.....	60
4.5.2 Square Wave (OSWV) Voltammetric Investigation Of Immunosensor	61
4.5.3 Differential Pulse Voltammetric Investigation Of Immunosensor.....	63
4.6 Development of Calibration curves	64
4.7 Real samples analysis:.....	69
4.7.1 Differential Pulse Voltammetric Investigation Of Immunosensor and Real Samples	69
4.7.2 Differential Pulse Voltammetric investigation of immunosensor and real sample.....	71
4.8 Electrochemical Impedance Spectroscopy (EIS) results	73
Conclusions	73
References	75

Chapter 1

1.1 Introduction

South Africa, as an arid country, is on the brink of serious water shortage crises. The low annual rainfall of less than 500 mm per annum, makes it one of the 30 driest countries in the world[1]. The provision of safe drinking water, for the burgeoning population, and to ensure economic sustainability, is proving to be a challenge for both the drinking water supplier's, the South African Government and business alike. The City of Cape Town Council has in recent years introduced water usage restrictions and water saving strategies to reduce the consumptive pressure on the dwindling water resources.

The limited natural water resource is placed under further pressure by the growing concern of Eutrophication. Eutrophication, or nutrient enrichment of water sources, is a direct consequence of human impact on the environment through urbanization and agricultural practices[2-3]. In developing countries, like South Africa, wastewaters from sewage and industries effluents in urban areas, which are often discharged in a poorly treated form or untreated in the environment, are increasingly becoming a major source of nutrients, causing eutrophication of surface water bodies[2]. Anthropogenic inputs of excess phosphorus and nitrogen that enters the water bodies, results in the water quality of surface water ecosystem becoming compromised, cause fish killings to occur and the

proliferation of algal growth [2, 4]. The most significant and well documented impact of Eutrophication is the global phenomenon of harmful algal blooms [5-7].

1.2 Harmful algal blooms

Harmful algal blooms occur where microscopic algae, that are naturally present in water systems, proliferate to such densities that they become visible to the naked eye. Most of these blooms are often dominated by Cyanobacteria, also known as blue-green algae[8]. Blue-green algae are able to dominate water systems owing to their unique ability to access spatially separated resources (light, nutrients, trace minerals). They possess gas vesicles which provide buoyancy and a mechanism to that allows them to control their vertical migration in the water column[9]. Cyanobacteria are photosynthetic bacteria found in surface waters all around the world and can occur in diverse habitats from fresh water to terrestrial soils. There is still a debate as to whether Cyanobacteria should be classified as an algae or bacteria. Cyanobacteria are prokaryotic, as they have no organized cell structures (like plasmids and mitochondria) thus they closely represent eukaryotic bacteria as opposed to algae[10]. They do also however have the capacity to photosynthesize owing to their pigments and photosynthetic mechanism. The names "cyanobacteria" and "blue-green algae" (Cyanophyceae) are valid and compatible systematic terms[9].

At least a third of the 50 known genera of cyanobacteria are capable of producing toxins and between 50 and 70 % of the blooms of those cyanobacteria are toxic[11]. Four potentially toxic genera are known for their ability to form massive blooms (*Anabaena*, *Aphanizomenon*, *Planktothrix* and *Microcystis*). In

South Africa, extremely dense scums of *M. aeruginosa* have been recorded with cell densities exceeding 10^9 cells/mL[12]. Thus the need for monitoring of algal toxins has become a necessity for the suppliers of drinking water. The City of Cape Town established the first dedicated municipal laboratory in South Africa for the undertaking of routine analysis for cyanotoxins in water supplies.

1.3 Cyanobacteria – Toxins

Cyanotoxins are classified based on the target organs they affect. The most common types of cyanotoxins are neurotoxins, such as the anatoxins and saxitoxins, and peptide hepatotoxins such as microcystins and nodularins[9]. Microcystins are the most widespread of all the cyanobacterial hepatotoxins and are produced mainly by cyanobacteria belonging to the genera *Microcystis*, *Anabaena*, *Planktothrix* and *Nostoc*. *Microcystis* genus is the most ubiquitous of the genera and produces the most commonly found hepatotoxins, called Microcystins. The species *M. aeruginosa* appears to be the most ubiquitous species producing toxic blooms[13]. In Cape Town, this species is responsible for seasonal blooms in some of the city's major source water dams. This occurrence usually takes place during summer when the water temperature, water pH, intensity of solar radiation, dissolved oxygen and CO₂ availability create the perfect bloom environment.

When cyanobacterial cells die, their cell walls burst, resulting in the release of the toxin into the water. The toxins are extremely stable and are not readily affected by breakdown chemical processes like hydrolysis or oxidation under conditions found in the most natural water bodies[13]. Microcystins have been shown to be

stable at low and high pH as well at extremely and high temperatures[9, 14]. Boiling water contaminated with microcystins does not break down the toxin. Microcystins have been found to persist in the environment under certain conditions for up to 30 days[15].

1.4 The chemical structure of Microcystins

Microcystins (MC's) are cyclic peptides containing seven amino acids, five non-protein amino acids and two protein amino acids. With more than 80 analogs, they are the most numerous of all the cyanotoxins and have been the focus of many researchers [9, 13, 16-19]. The molecular weight of microcystins and nodularins range from 800 to 1000 Daltons[20]. Microcystins (heptapeptides) (Figure 1) and Nodularins (pentapeptides) (Figure 1) are cyclic molecules, but have the same general structure namely:

cyclo-(D-alanine¹-X²-D-MeAsp³-Z⁴-Adda⁵-D-glutamete⁶-Mdha⁷) for
microcystins;

and cyclo-(D-MeAsp¹-L-arginine²-Adda³-D-glutamate⁴-Mdhb⁵) for Nodularin;

Where X and Z are the two variable L-amino acids; D-MeAsp is D-erythro-β-methylaspartic acid, Mdha is *N*-methyldehydroalanine and Mdhb is 2-(methylamino)-2-dehydrobutyric acid.

Adda is an unusual amino acid, unique to cyanobacterial toxins: (2S, 2S, 8S, 9S)-3-amino-9-methoxy-2,6,8-trimethyl-10-phenyldeca-4,6-dienoic acid[8-9, 21].

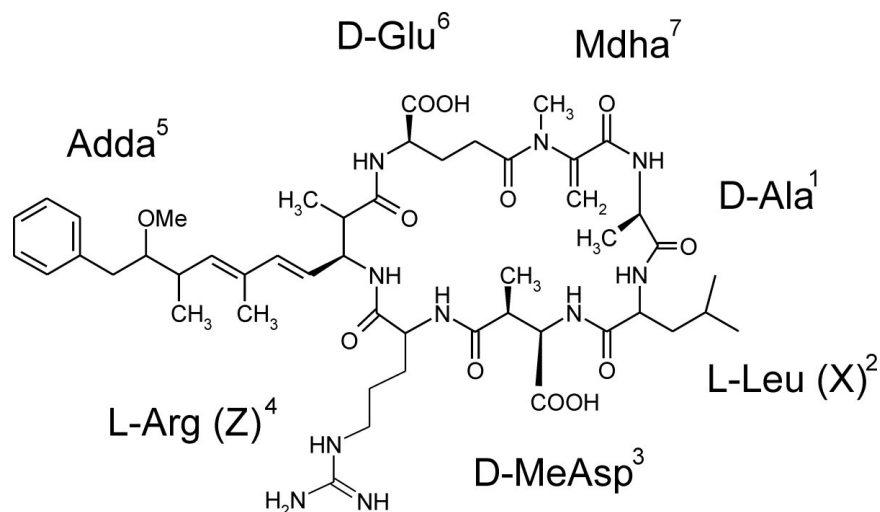


Figure 1. Structure of Microcystin-LR, where Z – Arginine and X - Leucine

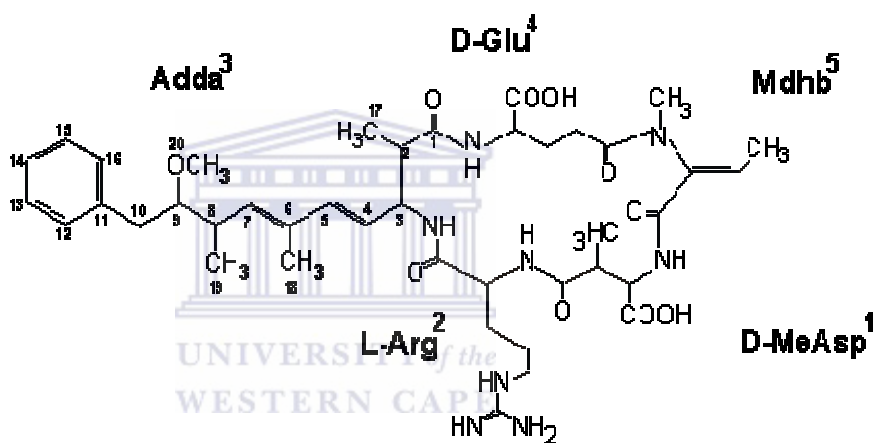


Figure 2. Structure of Nodularin

Different microcystins have different lipophilicities and polarities, which could affect their toxicity[22]. Microcystin-LR (MC-LR) was the first microcystin to be chemically identified and is possibly the most toxic representative of this group of hepatotoxins and is the subject of most of the cyanotoxin research [21, 23-25]. It has been associated with most of the incidents of toxicity involving microcystins in most countries [9, 22, 26].

The extreme toxicity of microcystins and nodularins (MCN's) has resulted in global efforts for rapid and economical detection methods. However, the potential of the misuse of MCN's in bioterrorist activities has led to stringent restrictions on the sale and transport of cyanotoxin standards. This control has limited the capacity for research, development of detection methods and monitoring of these algal toxins[27].

1.5 Toxicity of Microcystins & Nodularins (MCN's) and their Health Impacts

MCN's are affecting many organisms from micro-algae to mammals. MC-LR is known to paralyse *Chlamydomonas reihadtii*, a motile green alga, thus increasing its dominance in ecosystems by eliminating its competitors (reviewed in [8]). Zooplankton communities in lakes are also affected when microcystin-producing species dominate water ecosystems. While some Zooplankton (certain species of copepods) avoid ingesting *Microcystis* colonies, others species do ingest them and have the ability to bio-accumulate the toxins, while organisms like Daphnia have been shown to succumb to the toxins[8]. The bioaccumulation of toxins in lower organisms (mussels, crayfish, fish, frogs etc.) threatens the entire food web and ultimately humans that consume organism like fish [26, 28-29]. *Tilapia rendalli*, a fish used as a food source in Rio de Janeiro in Brazil, had MCN's in its muscle tissue when the levels of cyanobacteria were low [30-31]. These chronic low levels of toxins pose a health threat to humans.

In humans, the primary exposure route to cyanotoxins (MCN's) is via oral consumption of drinking water, contaminated food[32-33], or intake of water

during recreational activities, in contaminated water bodies[34]. The popularity of commercially produced algal foods as a health and dietary supplements has also been noted as a source of potential exposure to MCN's [18, 33]. MCN's cannot be taken up through the skin since the molecules are too large, however through dermal contact they can cause skin, eye and ear irritations, and in cases where swimmers swallow whole cells gastrointestinal symptoms such as vomiting and diarrhoea has been known to occur[22]. Human fatalities have occurred, the most renowned case occurred in 1996, where Brazilian haemodialysis patients at a dialysis centre, using municipal water supply water contaminated with cyanotoxins.

This was the first evidence for acute lethal human poisoning from MCN's[16] . Yuan *et al* reported that during this incident, 100 of 131 patients developed acute liver failure and 52 of these victims died as a result of the exposure and later confirm to be liver failure[35]. Detection and quantification of microcystins in these biological samples posed some analytical challenges since there were no well-established and routine analytic methods to measure total microcystins in tissue or sera samples[35].

The acute health effects of exposure to MCN's have received increasing attention around the world[9, 22], and has been well documented. MCN's are potent inhibitors of protein (serine/threonine) phosphatases PP1 and PP2a[34]. These enzymes remove the phosphate from protein and are a common biochemical process. This results in protein phosphorylation imbalances that cause the disruption of the cell structures, which in turn, results in death due to the hepatic

haemorrhage which occurs[25]. The liver cells die and disintegrate as the cellular cycles and structures are no longer maintained. Deformed hematocytes have also been observed in animal studies where they were exposed to microcystins [36-37]. By causing defective cells structures and disrupting cellular process like chromosomal division, it has been argued that MCN's may play a role in tumour promotion in the liver and colon[38]. The World Health Organization has thus made a provisional guideline for the exposure to microcystins. This risk is based on studies done with mice pigs exposed to microcystin-LR. Therefore a the guideline value of 1 µg/L for microcystin-LR is provisional, as the database is limited[22] .



1.6 Detection Methods for Monitoring of Microcystins & Nodularins.

Detection of cyanotoxins and in particular MCN's has gone through number improvements. The emphasis on increase sensitivity and the ability detect lower concentrations has been focus of many studies[39]. The analytical methods used for MCN's and specifically for Microcystin-LR can be divided into those that are used as screens i.e. they detect the presence of toxins and generally don't need pre-treatment of samples, and those that are used for the identification and quantification of various individual toxins and require elaborate and tedious pre-treatment and concentration steps.

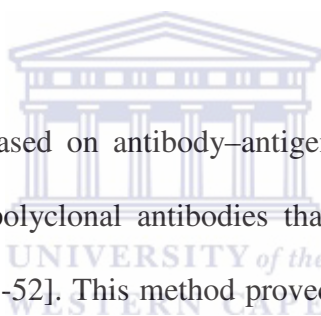
Screening techniques include the Mouse assay, enzyme-linked immunosorbent assay (ELISA), and the phosphatase bioassay. The mouse assay as a screening

tool is less desirable these days, yet it remains a reliable screening method giving results within a few hours[22]. It is able to distinguish between hepatotoxins and neurotoxins and provide information on the minimum amount of toxin to kill a mouse and compares this value with lethal doses of known amounts of toxin[9]. Several invertebrate bioassays ([40-42], plant bioassays [43-45] and *in vitro* methods [46] have been described for MCN detection.

The protein phosphatase inhibition assays (PPIA) is preferred by scientist as a screening tool as it times more sensitive than the HPLC. It is based on the inhibition of protein phosphatases by MCN's on a molecular level and shows comparable results for microcystin-LR equivalents with HPLC and ELISA [47-48]. Even though the method is relatively quick to perform and is sensitive to sub-nanogram levels of microcystins in treated water, the method is not specific to microcystins as it will detect other substances that inhibit protein phosphatases like okadaic acid[9, 26].

High-performance liquid chromatography (HPLC) with a photo diode array is the most precise method for the detection of hepatotoxins, but is limited by the availability of toxin standards[23]. The HPLC methods allows for the simultaneous determination of microcystin variants (LR, RR and YR). The disadvantages of HPLC methods are the time consuming process of pre-treatment of the samples to concentrate and purify the samples and elution time for each of the samples[49]. HPLC's coupled with UV detection are also limited due to the narrow absorption wavelength spectra of microcystins (between 200 and 300nm)[39] in which most variants occur. When HPLC is coupled with a mass

spectrometer, the molecular weights of the toxins gives rise to more accurate identification of microcystins[9]. Sangolkar *et al* reviewed newer advances in HPLC techniques that include the HPLC being coupled to electrospray ionization (HPLC-ESI-MS) and atmospheric pressure ionization (HPLC-API-MS) technologies[50]. However, the expensive equipment and running cost, as well as the requirement for highly trained personnel, make the HPLC methods difficult to maintain in large or small municipalities that do not have the financial freedom to do so. Perhaps the greatest disadvantage of this analytical method is the procurement of toxin standards particularly in third world countries like South Africa.



ELISA's methods are based on antibody-antigen interactions, these antibodies can be monoclonal or polyclonal antibodies that have been raised against the microcystin structure [50-52]. This method proved to be reliable in detecting and monitoring drinking water for MCN's [47] and has become a more affordable option to HPLC technologies. Commercially available ELISA kits are highly specific, sensitive and relatively quick to perform. The technical requirements are not as demanding as with the HPLC. Developments in ELISA have overcome shortcomings with the technique. Some ELISA used antibodies raised against specific toxins[53]. This is a limitation of some ELISA's since cross reactivity of the antibodies with different MCN's is variable and do not correlate with the type and toxicity of the molecules[47]. Fisher *et al* however has developed an ELISA that targets the ADDA portion common to all MCN's[54-55]. It reportedly detects all MCN's as it and was shown to have good cross sensitivity to the most common

types of microcystins (-LR,-RR, -YR,- LW,- LF,-LW, -LF, 3-desmethyl-MC-LR, 3-desmethyl-MC-RR, and Nodularin)[54]. The competitive indirect ELISA that Fischer et al developed consisted of synthetic ADDA-haptens, raising antibodies to ADDA showed low detection limits. An ADDA Elisa kit is available from Abraxis (Abraxis LLC, Product No. 520011).

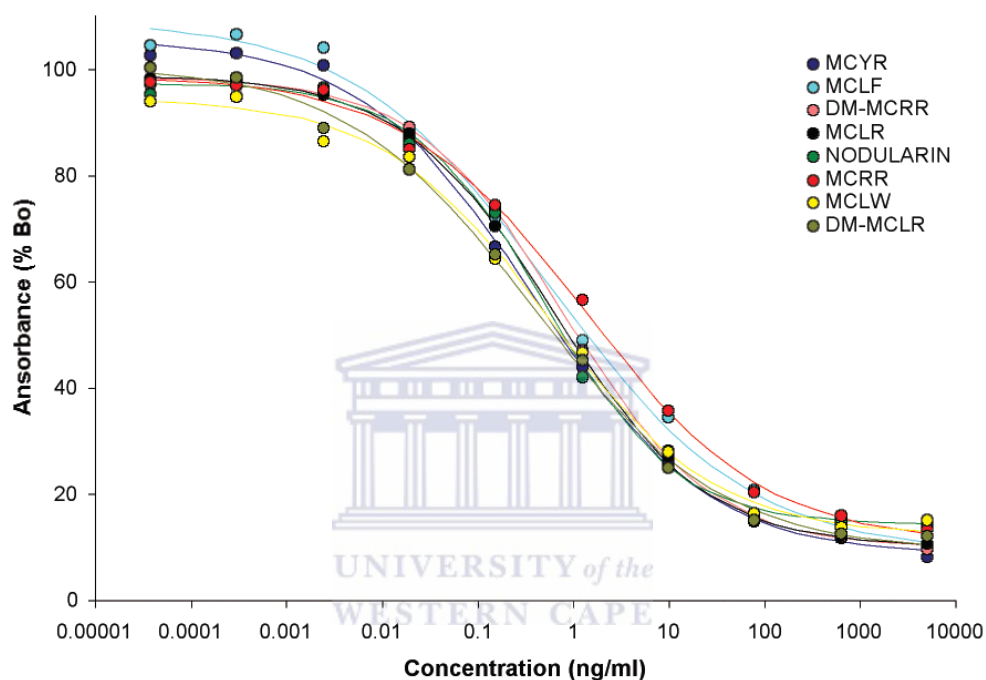


Figure 3. Abraxis ELISA standard curves showing good agreement between variants of Microcystins and Nodularins [54]

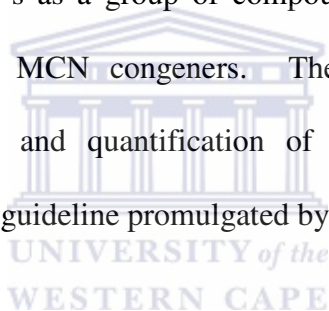
This product is robust, and can perform without sample pre-concentration, detects toxins in freshwater samples at lower concentrations than the phosphatase inhibition assay. It also shows good cross-reactivity with all cyanobacterial cyclic peptide toxin congeners tested to date[55]. The City of Cape Town uses this kit as its primary screen test and quantification for algal toxins in drinking water.

1.7 Human Risk to chronic exposure

The chronic exposure (long-term) to low dosages of MCN's in drinking water or recreational water or food products that has a potential for toxin bioaccumulation is a huge concern. The toxic mechanism of MCN's results in damage and it is not certain how much low-dosage damage occurs in humans before notable effects are visible. There is a risk of tumours associated with MCN's[22] and thus there is a need to be able to detect microcystins at even lower concentration than that of ELISA and PPIA's. Epidemiological studies in China have linked drinking surface water to increased liver cancer, and more recently to lower intestinal cancers [33_35]. There is presumptive evidence that the observed increase in liver cancer was linked with microcystin in the drinking water, and the high cancer rates have been successfully reversed by provision of drinking water wells. Laboratory studies with Nodularin and with microcystin-LR have shown possible carcinogenesis, though this needs to be confirmed using standard procedures for carcinogenesis testing [36, 37]. Continuous low level exposure to microcystins may also result in hepatic accumulation; researchers have found that microcystin excretion occurs very slowly[56]. Bioaccumulation of toxins have been demonstrated in the livers of animals[31, 57-58], these results raises a serious concern for that long term exposure to even very low levels of microcystins may be significant. The prevalence of liver cancer and other liver diseases may become more prevalent as drinking water suppliers struggle with a growing problem of cyanotoxin blooms [37, 59].

Newer detection techniques with greater sensitivity are being researched and developed. Biosensors are at the forefront of the research into detecting toxins in the environment.

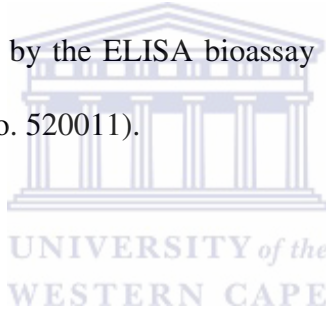
This present work aims to develop an immunosensor that is cost effective and easy to produce. We endeavour to develop an immunosensor for the detection of Microcystins and nodularins using anti-sheep IgG antibody immobilised on a modified glassy-carbon polymer surface. The immunosensor will be applied to water samples for MCN's as a group of compounds recognised by the ADDA moiety common to all MCN congeners. The immunosensor will provide immediate confirmation and quantification of MCN's in situ at very low concentration, below the guideline promulgated by the WHO (1 µg/L).



Chapter 2

2.1 Introduction:

This section summarises the findings of the results of microcystin monitoring results undertaken at Voëlvlei Water Treatment Works near Gouda and, to lesser extent results, from Faure Treatment Works. The Treatment works treats raw water stored in Voëlvlei dam and provides this treated potable water via a pipeline to the citizens Cape Town. Weekly toxin tests are performed as part of a mandatory monitoring programme to ensure the water provided is safe for public consumption. The monitoring of Algal toxins, specifically microcystins and nodularins is undertaken by the ELISA bioassay (Abraxis ADDA Elisa kit from Abraxis LLC, Product No. 520011).



The concerns over the health risks and impacts that cyanotoxins pose to people prompted the World Health Organization (WHO) to adopt a provisional guideline, based on a value for microcystin-LR, in drinking water[9, 22]. Due to the lack of reliable analytical data, no guideline values have yet been set for the concentrations of nodularin or to other toxins (cylindrospermopsin, anatoxin etc) in water[22]. Currently, many countries are using the WHO guideline of 1 µg/L of Microcystin equivalents as a guide to monitoring their drinking water sources [19, 27, 38].

In South Africa specific the SANS 241 (2011) stipulates the guideline for drinking water standards with respect to comes to cyanotoxins, specifically microcystins. Guidelines value has, however, been not been set for the maximum permissible concentration for cyanotoxins in recreational water.

The Department of Water Affairs (DWA) guidelines of 1996 contain the following table:

Table 1. The effects of Microcystin on Human Health

Microcystin Range (µg/L)	Effects
<i>Target Water Quality Range</i> 0 - 0.8	<i>No health effects expected</i>
0.8 - 1	Possible chronic effects associated with the long-term ingestion of microcystins in the drinking water.
> 1	Possible acute hepatotoxic effects

2.2 Algal Monitoring in the City of Cape Town

Algal monitoring plays an important role in the monitoring of our raw drinking waters and potable water systems. Nuisance algal levels in drinking water dams are an ever increasing global concern. The shift in many algal communities is towards the dominance of the Blue-Green algae (Cyanophyceae) as a result of nutrient enrichment (eutrophication). Some of these species have the ability to

produce toxic blooms which poses a real threat to humans and animals. Scientific Services Branch, City of Cape Town, regularly monitors drinking water (potable and raw water) and recreational water bodies for the presence of harmful algae species.

Prior to 1995 the only algal monitoring simply amounted to using microscope to identify and count algae in water samples. The species composition and relative abundance of the different species in the sample gives an indication of whether any problem species are beginning to dominate in a water body. The measuring of chlorophyll-*a* concentration of the sample also helped as an indication of the amount of algae in the water body. When the abundance of algal cells exceeded accepted guidelines, the next step was to test the sample for the presence of toxins called microcystins.



Since 1995, toxin analysis was done by High Performance Liquid Chromatography (HPLC) method (Figure 4). A large volume (2L) of sample was required. The samples had to be filtered and then taken through an extraction process for between 8 to 24 hours. This step was then followed by a further process during which the sample is blown down using N₂ gas to concentrate the sample to a new volume. Sample concentration is the major pre-treatment draw back High Performance Liquid Chromatography (HPLC) to determine the concentration of the different variants of toxins. The entire process described above takes approximately 1¹/₂ days before a result can be obtained. Since 2005, the City invested in ELISA instrumentation (Figure 5) and embarked on staff training in the ELISA method for toxin analysis. ELISA, or Enzyme-Linked

Immunosorbent Assay, is an immunoassay technique involving the reaction of antigen and antibody in vitro. ELISA is a sensitive and specific assay for the detection and quantitation of antigens or antibodies. ELISA tests are usually performed in microwell plates. The sensitivity of Elisa's allows for lower detection limits of toxins than HPLC's.

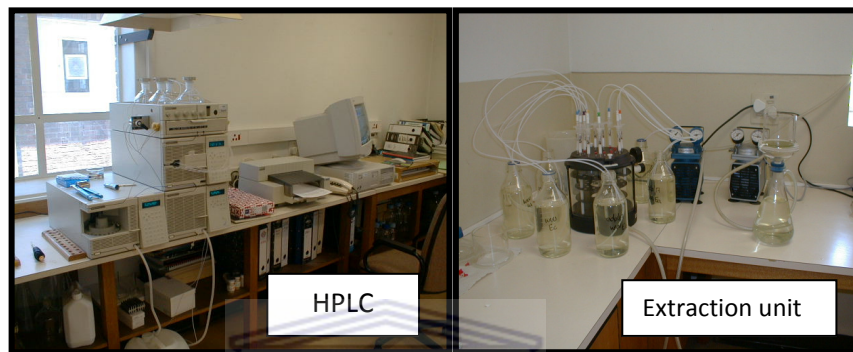


Figure 4. HPLC and Extraction unit used to concentrate toxins in raw water



Figure 5. ELISA Reader, kit contents and micro well plates

ELISA results can be reported within 2-3 hours of sample receipt. Multiple samples can be run simultaneously (in contrast to the hourly samples of the HPLC).

Table 2. Comparison of HPLC and ELISA methods for Toxin Analysis

	HPLC	ELISA
Time	1 ¹ / ₂ days for a results	2 hours for a result
Cost	+/- R1500 per sample	+/- R800 and cheaper if multiple samples are run
Detection limits	0.5 µg/L	0.1 µg/L
Toxins	Microcystin variants	Microcystin and Nodularin variants
Number of samples	1 sample run at a time	Simultaneous Multiple samples: up to 41 samples in duplicate

2.3 Enzyme-Linked Immuno-Sorbent Assays

Enzyme-linked immune-sorbent assay (ELISA) is a biochemical technique used mainly in immunology to detect the presence of an antibody or an antigen in a sample. ELISA's is an immunoassay that exploits the specificity between antibodies and antigens. The origins of ELISA's began in 1945 when the concept of immunoassays was first described, and followed a series' of developments through to 1972 when Engvall and Perlman introduced the use of enzymes as labels for immunoassay, they first coined the term enzyme-linked immunosorbent assay (ELISA) (cited in[60]). Since then the development and advantages of immunoassays has received a lot of attention. The ELISA has been used as a diagnostic tool primarily in medicine and plant pathology, as well as a quality control check in various industries[61-62]. Simplistically stated, in ELISA an unknown amount of antigen or antibody is affixed to a surface (eg. A microwell plate), and then a specific antibody or antigen is washed over the surface so that it

can bind to the corresponding antigen or antibody. This antibody or antigen is linked to an enzyme, and in the final step a substance is added that the enzyme can convert to some detectable signal. There are, however, a variety of formats of ELISA's each with advantages and disadvantages. Table 3 shows the steps and variety of the different types of ELISA's



Table 3. Measuring Principles for ELISA Types (from Biosense)

Process	Indirect Sandwich	Direct Sandwich	Direct Competitive Antigen Capture	Direct Competitive Antibody Capture	Indirect Competitive Antibody Capture
Immobilization reaction	A capture antibody binding specifically to the analyte (antigen) is immobilized on a solid phase (microtiter plate well).	A capture antibody binding specifically to the analyte (antigen) is immobilized on a solid phase (microtiter plate well).	An antibody binding specifically to the analyte (antigen) is immobilized on a solid phase (microtiter plate well, polystyrene tube or magnetic particles).	A standard analyte (antigen) is immobilized on a solid phase (microtiter plate).	A standard analyte (antigen) is immobilized on a solid phase (microtiter plate well).
Binding of analyte	The sample is added, and the analyte in the sample binds to the capture antibody on the solid phase. Unbound components are washed away.	The sample is added, and the analyte in the sample binds to the capture antibody on the solid phase. Unbound components are washed away.			
Binding of detection antibody	A detecting antibody binding specifically to the analyte is added, creating a sandwich. Unbound detecting antibody is washed away.				
Competition reaction			The sample is added together with an enzyme-labelled standard ("tracer"). The "tracer" competes with the analyte in the sample for binding to the antibody on the solid phase. Unbound components are washed away.	The sample is added together with an enzyme-labelled antibody specific for the analyte. The analyte in the sample competes with the standard analyte on the solid phase for binding to the antibody. Unbound components are washed away.	The sample is added together with a primary antibody specific for the analyte. The analyte in the sample competes with the standard analyte on the solid phase for binding to the antibody. Unbound components are washed away.
Binding of enzyme-labelled antibody	An enzyme-labelled antibody binding specifically to the detection antibody is added. Unbound antibody is washed away.	An enzyme-labelled detecting antibody binding specifically to the analyte is added, creating a "sandwich". Unbound detecting antibody is washed away.			An enzyme-labelled antibody binding to the primary antibody is added. Unbound antibody is washed away.
Chromogenic reaction	A non-coloured substrate is added, and the substrate is converted to a coloured product by the enzyme bound to the antigen-antibody complex.	A non-coloured substrate is added, and the substrate is converted to a coloured product by the enzyme bound to the antigen-antibody complex.	A non-coloured substrate is added, and the substrate is converted to a coloured product by the enzyme bound to the solid phase.	A non-coloured substrate is added, and the substrate is converted to a coloured product by the enzyme bound to the analyte-antibody complex.	A non-coloured substrate is added, and the substrate is converted to a coloured product by the enzyme bound to the antigen-antibody complex.
Quantitative analysis	The colour intensity is measured with a microplate reader and the absorbance is directly proportional to the concentration of the analyte in the sample. The relationship between absorbance and analyte concentration is obtained from a standard curve created from a reference material.	The colour intensity is measured with a microplate reader and the absorbance is directly proportional to the concentration of the analyte in the sample. The relationship between absorbance and analyte concentration is obtained from a standard curve created from a reference material.	The colour intensity is measured with a microplate reader or a spectrophotometer and is <u>inversely</u> proportional to the concentration of the analyte in the sample. The relationship between absorbance and analyte concentration is obtained from a standard curve created from a reference material.	The colour intensity is measured with a microplate reader and is <u>inversely</u> proportional to the concentration of analyte in the sample. The relationship between absorbance and analyte concentration is obtained from a standard curve created from a reference material.	The colour intensity is measured with a microplate reader and is <u>inversely</u> proportional to the concentration of analyte in the sample. The relationship between absorbance and analyte concentration is obtained from a standard curve created from a reference material.

Adapted from Biosense : Biosense Laboratories AS Thormøhlensgt. 55 Bergen, N-5008, Norway Tel:(+47) 55543966; Fax:(+47) 55543771 ; E-Mail: biosense@biosense.com

formats[61]. From Table 3 above, it is clear that both direct and indirect ELISA can be used for antigen (or antibody) detection, the indirect ELISA is more common as this format of ELISA utilizes a primary antibody in conjunction with a labelled secondary antibody. Since the labelled secondary antibody is directed against all antibodies of a given species (e.g. anti-sheep), it can be used with a wide variety of primary antibodies (e.g. all sheep monoclonal antibodies)[63]. The use of secondary antibody also provides an additional step for signal amplification, increasing the overall sensitivity of the assay[60]. Direct methods also lack the additional signal amplification that can be achieved with the use of a secondary antibody[63].

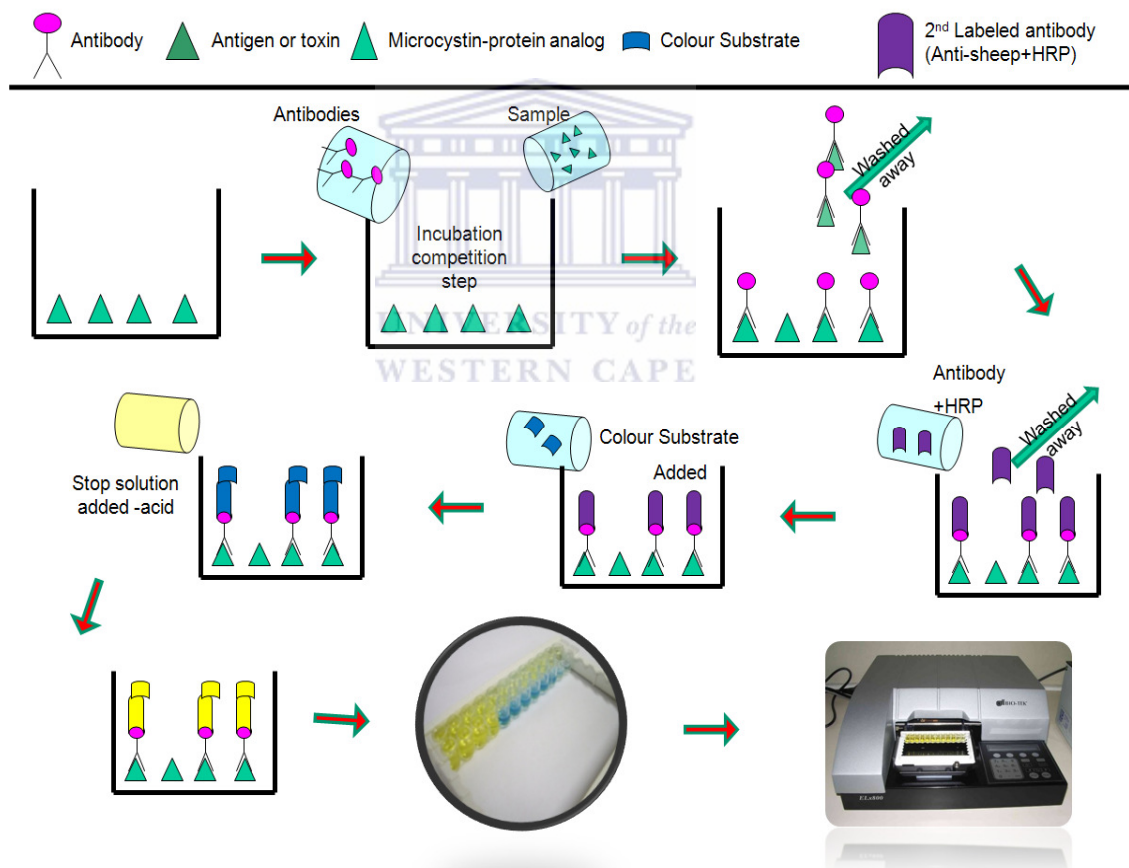
2.4 An ADDA Elisa kit is available from Abraxis

The ADDA ELISA Kit (Abraxis LLC, Product No. 520011) is an enzyme-linked immunosorbent assay for the congener independent determination of microcystins and nodularins in water samples. The assay utilizes polyclonal antibodies that have been raised against the ADDA moiety of the molecule, allowing for the detection of microcystins and nodularin variants (over 80 variants are currently known) in drinking, surface, and groundwater at levels below World Health Organization (WHO) guidelines[55].

The recognition of microcystins, nodularins and their variants by a polyclonal sheep antibody is the bases of this indirect competitive ELISA[54]. When present in a sample, microcystins and nodularins compete with a microcystins-protein analog that is immobilized on wells of a microtiter plate for the binding sites of antibodies in solution. After a washing step, a second labelled antibody is added and incubated, antibody- Horseradish Peroxidase (HRP). After a washing step and

addition of a substrate/chromogen solution, a colour signal is generated. The intensity of the colour is inversely proportional to the concentration of the microcystins/nodularins present in the sample. The colour reaction is stopped after a specified time and the colour is analysed using a microwell plate spectrophotometer to obtain the optical density (OD) at a wavelength of 450 nanometer (nm)[64]. Various software packages are available to calculate the concentrations (eg GEN5 [65]) Below is a schematic of the ADDA ELISA process.

Figure 6. Schematic Representation of the ADDA Indirect Competitive ELISA



The ADDA ELISA Test Kit (**Figure 7**) contains:

- A Microtiter plate coated with an analog of microcystins conjugated to a protein;
- Standards (6) : 0ppb ; 0.15 ppb; 0.40 ppb; 1.0 ppb; 2.0 ppb; and 5.0ppb

Figure 7. Abraxis ADDA ELISA kit



- A Positive control with a concentration of 0.75 ppb;
- Antibody solution (polyclonal anti-Microcystins);
- Anti-Sheep-HRP Conjugate;
- Wash Solution 5X Concentrate;
- Colour Solution, tetramethylbenzidine (TMB);
- Stop Solution;
- Diluent/zero solution, 25 mL

2.5 Findings of ELISA data collected from raw water, Cape Town.

Weekly samples from different treatment works supplying the City of Cape Town are delivered for toxin analysis by ELISA - ADDA (Abraxis) bioassay. To improve toxin quantification, in the raw water samples, algal cells need to be lysed. This can be achieved by freeze thawing or sonication[9]. Samples were pre-treated by sonication to effect lysis of the cells in a small Elma sonication water bath at approximately 78°C to 80°C [9]. The total microcystins and nodularins present (intra- and extracellular toxins) will thus be determined. Elisa can be validated by HPLC as it compares favourably.

The results of ongoing algal toxin monitoring of drinking water at two treatment works are presented below in Table 4. The mean and maximum values of MCN's tested via ELISA method was determined for the period July 2007 to March 2011.

Table 4. ELISA summary results for Faure and Voëlvlei waters.

Water Source	Mean Value (µg/L MC-LR)	Maximum value (µg/L MC-LR)
Faure Treatment Works: Firlands Raw water (n=11)	0.12	0.27
Faure Treatment Works: RSE Raw water (n=41)	0.15	0.27
Voëlvlei Treatment Works: Raw water (n=113)	0.17	0.94
Voëlvlei Treatment Works: Treated water (n=99)	0.13	0.31

The mean values of the raw and treated water remain below the 0.2 µg/L level. The values less than 0.15 µg/L have been reported as <0.15 µg/L as this is the lowest standard in the Abraxis ADDA Elisa kit. The kit did not show the good consistency when detecting lower values of antigens. The manufacturers reported detection limits of quantitation to be 0.02 µg/L to 0.07 µg/L[54]. This was difficult to achieve in the routine analysis performed on the drinking water samples from Voëlvlei and Faure treatment works. The maximum values for the periods sampled indicate that Faure works does not support large numbers of algal cells. However, the Voëlvlei works shows a propensity for supporting harmful algal blooms. During this period of data review no significant outbreak of blue green algae blooms occurred, but prior to 2006, Voëlvlei Dam did produce blue green algal blooms. This incident, however, was not tested with the ELISA ADDA kit being discussed. The blooms resulted from poor quality water that was added to the dam from the Klein Berg River to augment the dam levels. The Klein berg river is impacted by the agricultural town of Tulbugh. The maximum values in Table 3 above, are below the WHO guideline of 1µg/L thus this water is deemed as being safe for consumption.

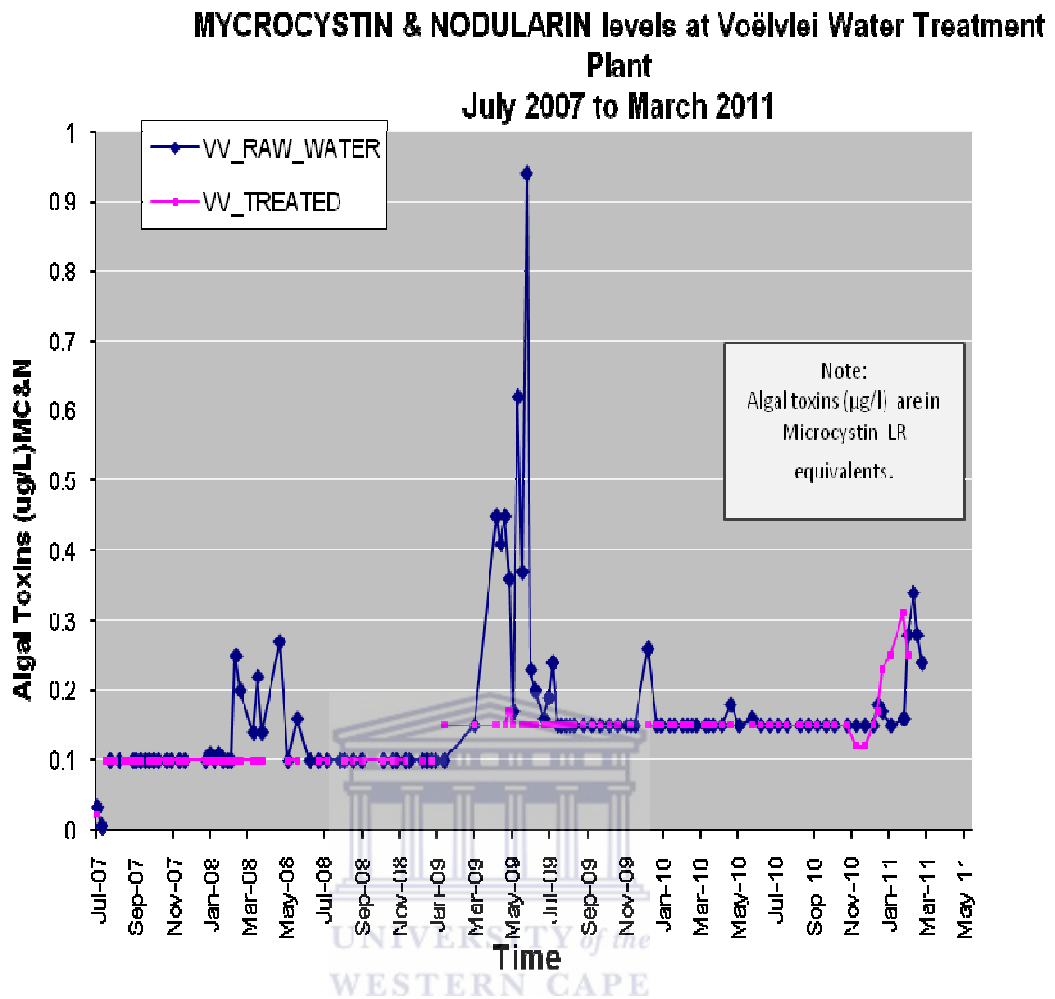


Figure 8. Time series showing trends of ELISA toxin data at Voëlvlei Water Treatment Works

The trend graph at Voëlvlei Dam (Figure 8) shows that for most of the time the toxin levels in the raw waters are below the detection limit of 0.15 $\mu\text{g/L}$ and that the treatment process does clean up toxins to below this level as well. The raw water trend indicates that during the summer months there is an increased level of toxin concentration present in the water. Managers of treatment works are critically aware of this and do prepare for bloom events by having powdered activated carbon in their stores as a means of removing the toxins if the levels

should overshoot the WHO guideline. Thus it would appear that there is a low level presents of toxin present all year round and peaks during the summer months when condition for algal growth are optimal. Low level of toxin exposure or to rephrased low level chronic exposure to MCN's in the water is not well known, especially for humans. As a potent inhibitor of protein phosphatase 1A and 2A activities, MCN's are similar to okadaic acid as, known tumour promoter [22]. In China it was found that the primary liver cancer prevalence was associated with drinking water contamination [59]. Zhou *et al* also should that there an was an association between the incidence of colorectal cancer and drinking water, which may be related to low level chronic exposure to microcystins and nodularins in drinking water[66]. The reliable early and cost effective detection of microcystins is being pursued by many researchers so that lower chronic level toxin can be more accurately measure. ELISA's are probably the most widespread immunochemical method and several diagnostic ELISA kits are now commercially available [39]. Pyo *et al.* 2005a integrated an ELISA into a microchip [67]. Also various biosensors employing antibodies [68-69] have been constructed and represent promising technologies especially for routine monitoring of environmental waters. Other detection techniques involve specific artificial receptors (molecularly imprinted polymers), which have been recently designed for microcystin-LR[70]. They have been employed not only for SPE sample clean-up, but also for construction of sensitive and inexpensive competitive assays or biosensors for microcystins analysis [71-72].

In this study we will look to develop an inexpensive easy to assemble biosensor (immune-sensor) for MCN's. The definition of a biosensor is generally accepted in literature as a self contained integrated device consisting of a biological recognition element (enzyme, antibody, receptor or micro-organism) which is interfaced to a chemical sensor (i.e. analytical devise) that together reversibly responds in a concentration-dependant manner to a chemical species.



Chapter 3

This chapter addresses the various analytical electrochemistry techniques and materials used in this current study in the development of the immunosensor for the antibody-antigen based detection of microcystin and nodularin toxins in water.

Methodology

3.1 Electrochemistry

Electrochemistry analytical methods are a class of techniques in analytical chemistry which study an analyte by measuring the potential (volts) and/or current (amperes) in an electrochemical cell containing the analyte [73]. These methods can be broken down into several technique-categories depending on which aspects of the cell are controlled and which are these various aspects are to be measured. The study of voltammetry, where the electrochemical cells current is measured while the cells potential is actively changing is the most common technique used. Another technique that is also commonly use is the impedimetric techniques.

Voltammetry developed from the discovery of polarography in 1922 by the Czech chemist Jaroslav Heyrovsky, for which he later received the Nobel Prize in chemistry [74]. In the 1960s and 1970s significant advances were made in all areas of voltammetry (theory, methodology, and instrumentation), which enhanced the sensitivity and expanded the repertoire of analytical methods[73].

The application of a potential (E) to an electrode and the monitoring of the resulting current (i) flowing through the electrochemical cell is a common characteristic of all voltammetric techniques [74]. In many instances the applied

potential is varied or the current is monitored over a period of time (t). Thus voltammetric techniques can be described as some function of E , i , and t . They are considered active techniques because the applied potential forces a change in the concentration of an electroactive species at the electrode surface by electrochemically reducing or oxidizing it, this is different to the passive techniques such as potentiometry[73].

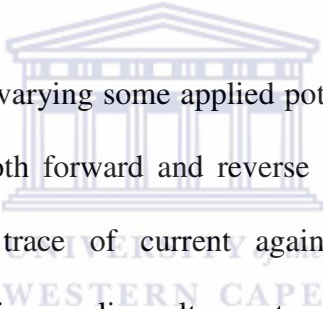
Voltammetric techniques have the analytical advantages in that they have better sensitivities with a very large useful linear concentration range for both inorganic and organic species (10^{-12} to 10^{-1} M), a large number of useful solvents and electrolytes, a wide range of temperatures, rapid analysis times (seconds), simultaneous determination of several analytes, the ability to determine kinetic and mechanistic parameters, a well-developed theory and thus the ability to reasonably estimate the values of unknown parameters, and the ease with which different potential waveforms can be generated and small currents measured [74].

Voltammetric techniques are often used for the quantitative determination of a variety of dissolved inorganic and organic substances. However, the use of voltammetric techniques has been applied to a variety of purposes, including fundamental studies of oxidation and reduction processes in various media, adsorption processes on surfaces, electron transfer and reaction mechanisms, kinetics of electron transfer processes, and transport, speciation, and thermodynamic properties of solvated species. Voltammetric methods are also applied to the determination of compounds of pharmaceutical interest and, when

coupled with HPLC, they are effective tools for the analysis of complex mixtures[73].

3.1.1 Cyclic voltammetry

Cyclic voltammetry is a widely used electro-analytical technique that uses micro-electrodes and unstirred solution so that measured current is limited by the analyte diffusion at the electrode surface. It has wide applications in the study of redox processes, electrochemical properties of analytes in solution and for understanding reaction intermediates as well as for obtaining the stability of reaction products [73-74]



The technique works by varying some applied potential at a working electrode at some scan rate (ν) in both forward and reverse direction while monitoring the current. The resultant trace of current against potential is termed as a voltammogram[74]. During cyclic voltammetry measurement, the potential is ramped from an initial potential, E_i to a more negative or positive potential but, at the end of the linear sweep, the direction of the potential scan is reversed, usually stopping at the initial potential, E_i (or it may commence an additional cycle)[74]. The potential is usually measured between the reference electrode and the working electrode and the current is measured between the working electrode and the counter electrode (auxiliary electrode)[75].

A typical cyclic voltammogram is illustrated in figure 9.

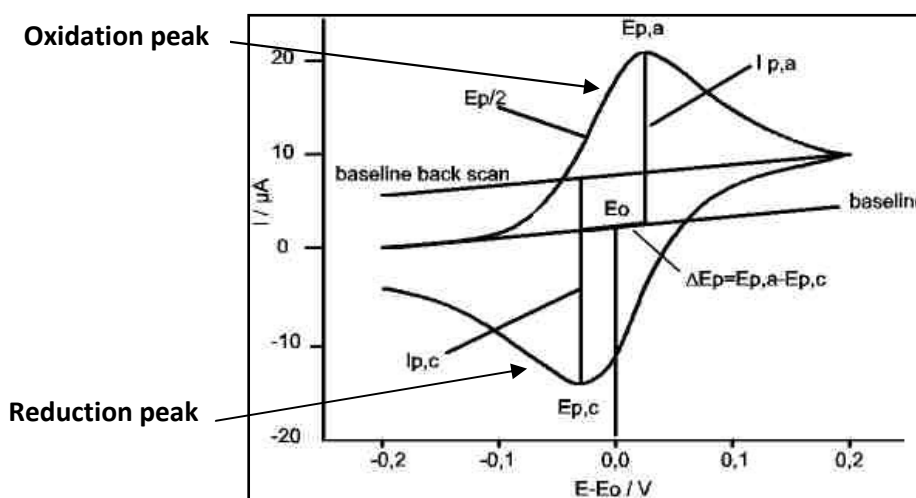


Figure 9. Typical cyclic voltammogram showing reduction and oxidation peaks

Important parameters and information are usually obtained from cyclic voltammograms for analysis of redox properties of an electroactive sample. These parameters include

- Peak potentials (E_{pc} , E_{pa}) and peak currents (I_{pc} , I_{pa}) of the cathodic and anodic peaks, respectively.
- It also provides information about the sample
- The reversibility or irreversibility of the reaction or whether it is quasi-reversible.
- insight into how fast the electron process is, relative to other processes such like diffusion.[74]

3.1.2 Square wave voltammetry

Square wave voltammetry (OSWV) is an improvement and on the linear sweep voltammetry because it allows for a more sensitive interrogation of the electrochemical nature of the analytes. In linear sweep voltammetry (as mentioned above) where the current at a working electrode is measured while the potential between the working electrode and a reference electrode is swept linearly in time.

In OSWV a square wave is superimposed on the potential staircase sweep so that peaks and troughs that are recorded during the square wave sweep occurs at the potential where the chemical species present is either oxidised or reduced. The potential sweep in OSWV is a series of stair steps; therefore the current is measured at the end of each potential change and before the next, so that the contribution to the current signal from the capacitive charging current is minimized[73-74]. The advantages of the OSWV technique are more sensitive and therefore have much lower detection limits due to the lower contribution of capacitive of charging current[76]. Detection limits for SWV are on the order of nanomolar concentrations and the scan times are much faster.

3.1.3 Differential Pulse Voltammetry

Differential Pulse Voltammetry (DPV) is similar to linear sweep voltammetry in that the potential is scanned with a series of pulses, however the difference is that each potential pulse is fixed and of small amplitude (10 to 100 mV), and is superimposed on a slowly changing base potential[76]. Current is measured at two points for each pulse, the first point just before the application of the pulse and the second at the end of the pulse. These sampling points are selected to allow for the decay of the non-faradaic (charging) current. The difference between current measurements at these points for each pulse is determined and plotted against the base potential[74].

DPV is a useful technique for identifying any electroactive specie at the working electrode surface. This technique is suited for characterizing thin conducting polymer films. The potentials of the peaks formed with DPV, can help to identify

the cation in solution. The concentration of analytes can also be determined with DPV since the peak area is proportional to concentration. When using the Osteryoung-parry equation, the peak height can be used to estimate the analyte concentration in solution[73-74].

The equation is

$$\Delta I_p = (n^2 F^2 A / 4RT) \cdot (D/\pi t)^{1/2} \cdot C_{\text{analyte}} \Delta E$$

where

I_p = Peak current for either the oxidation or reduction peak being considered

n = Number of electrons transferred

F = Faraday constant (96584 C mol⁻¹)

Γ^* = Surface Concentration of the electroactive film bound to the working electrode.

A = Surface area

ν = Scan rate (Vs⁻¹)

R = Gas constant (8.314 Jmol⁻¹K⁻¹)

T = Temperature the system (K)

D = Diffusion coefficient

t = is the time between pulses.

The magnitude of ΔE and the rooted term $(D/\pi t)$, implies that the separation of potential and diffusion of analyte to the electrode plays an important role in determining the value of ΔI_p which increases the accuracy of this technique. By working with a differential current the sensitivity of the technique is improved.

3.2 Electrochemical Impedance Spectroscopy (EIS)

3.2.1 Background

EIS is widely used as a standard characterization technique for many material systems and applications (e.g. corrosion, plating, batteries, and fuel cells)[77]. Simply stated it is the response of an electrochemical system or cell to an applied potential. In cyclic voltammetry and other dynamic electroanalysis, an applied potential is either constant (potentiostatic) or changing (potentiodynamic) when ramped at a constant rate of $v = dE/dt$ [74]. However, in impedance, a small perturbing potential (~ 5 mV amplitude[77]) is applied across a cell or sample and changes in a cyclic sinusoidal manner and generates a current resulting from the overpotential (η) caused by the small displacement of the potential from the equilibrium value. Over a time scale, the averaged over potential is zero. Because the potential is only perturbing, it has the advantage of minimizing the concentration change after the experiment. The induced current alternates because the voltage changes in a cyclic manner, hence the term alternating current (AC). Impedance is therefore a measure of the ability of a circuit to resist the flow of an alternating current (AC)[74, 78]. It is synonymous to resistance (R) used in direct current (DC), which is defined by Ohm's law

$$R = E / I$$

as the ratio between voltage (E) and current (I)[73-74].

The advantages of EIS are that it is a non-destructive and rapid in situ technique for examining processes occurring at the electrode surface. During a controlled-potential EIS experiment, the electrochemical cell is held at equilibrium at a fixed DC potential, and a small amplitude (5–10 mV) AC wave form is superimposed

on the DC potential to generate a response from the equilibrium position. The response to the applied perturbation, which is generally sinusoidal, can differ in phase and amplitude from the applied signal. This response is measured in terms of the AC impedance or the complex impedance, Z (overall or complete impedance), of the system, which permits analysis of electrode process in relation to diffusion, kinetics, double layer, coupled homogeneous reactions, etc [79]. The complex impedance (Z^*) is made up of a resistive or real part Z' , attributable to resistors (in phase with the applied voltage), and a reactive or imaginary part Z'' , attributable to the contributions of capacitors. This is related to the resistance (R), reactance (X) and capacitance (C) by the equation:

$$Z^* = R - jX$$

where $X = 1/\omega C$ and $\omega = 2\pi f$. R is the resistance measured in Ohms (Ω), X is the reactance, C the capacitance measured in Farads (F), ω the applied angular frequency measured in rad s^{-1} and f is the frequency measured in Hertz (Hz)[73].

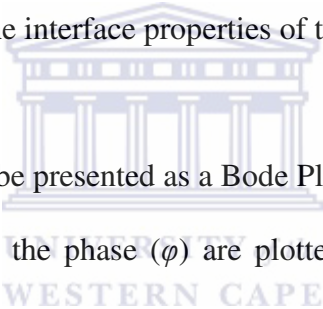
Notational representation of this in terms of Z' and Z'' is given by:

$$Z^* = Z' - jZ'' \text{ where } j = \sqrt{-1}$$

Because Z^* is defined by the complex term, j , which determines the contribution of Z'' to Z' , the term complex impedance is often used. For a pure resistor that is not having any capacitance, its resistance when determined with a continuous current (DC) is R because its impedance is frequency independent, $Z^* = Z' = R$ [74].

3.2.2 Nyquist & Bode Plots

The Nyquist plot of Z' is often used to present experimental data collected from an impedance experiment (usually positive x-axis corresponds to the real impedance), versus Z'' (usually, the positive y-axis correspond to $-Z''$), over a wide frequency range (100 kHz to 0.1 Hz). The Nyquist plot of impedance spectra includes a semicircle portion and a linear portion, with the former at higher frequencies corresponding to the electron transfer process and the latter at lower frequencies corresponding to the diffusion process. The electron transfer resistance (R_{ct}) at the electrode surface is equal to the semicircle diameter, which can be used to describe the interface properties of the electrode[74, 80].



Impedance data can also be presented as a Bode Plot in which the logarithm of the absolute value of Z' and the phase (φ) are plotted against the logarithm of the frequency (f)[81]. This can be plotted on the same axis or separately. The data in Nyquist plots is often poorly resolved (particularly at high frequencies), but are more commonly displayed for historical reasons. The explicit frequency dependence is not displayed in the Nyquist plot. In contrast, the bode plot directly displays the frequency dependence; in addition, the data is well resolved at all frequencies, since a logarithmic frequency scale is used. When the frequency of the AC waveform is varied over a wide range of frequency (ca about 10^{-4} and $> 10^6$ Hz), the impedance obtained for the system is a function of the operating frequency. Spectra of the resulting impedance at different frequencies do reveal the different electrochemical kinetics involved in the system. While dipolar

properties are manifest at the high frequency regions, bulk and surface properties will be evident at intermediate and low frequencies respectively[81].

The total impedance of a system is determined by the various component impedances of an electrochemical cell; for example, electron transfer kinetics, diffusion and passivating layers. The relative contribution of the various components typically varies with frequency; for example, electron transfer kinetics may dominate at high frequencies, whereas diffusion may dominate at lower frequencies[81].

Thus to characterize impedance, Z , the following must be specified; its magnitude, absolute Z' , phase angle, (ϕ), and the frequency, f (in cycles per second, or Hertz), at which it was measured. These three parameters are represented as the Bode plot (Figure 10(a)). The plot of the real part of impedance against the imaginary part gives a Nyquist Plot (Figure 10(b)). The shape of the resulting curve (or semicircle) is important in making qualitative interpretations of the data. Electrochemical Impedance plots sometime contain several semicircles and often only a portion of the semicircle is seen. Both plotting formats are used because each has its strengths. The advantage of Nyquist representation is that it gives a quick overview of the data and one can make some qualitative interpretations [79]. The disadvantage of the Nyquist representation is that one loses the frequency dimension of the data. One way of overcoming this problem is by labelling the frequencies on the curve.

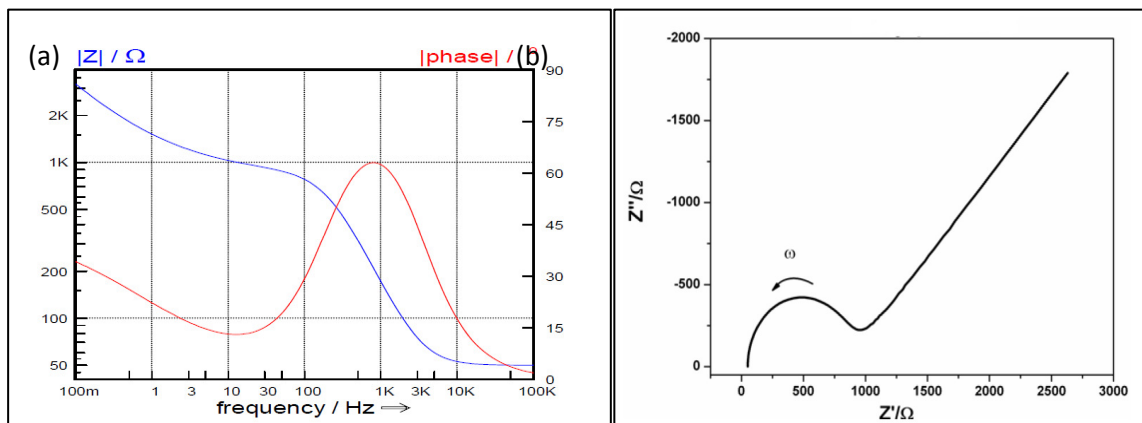


Figure 10. Typical Bode Plot (a) and a typical Nyquist Plot (b)

To quantitatively analyze the data from the Nyquist or Bode plot, it has to be fitted to an equivalent circuit where the values of the electrical components are associated with the physical/ chemical properties of the electrochemical system being studied. The circuit model provides a simple way of understanding what may be a complicated electrochemical system. The equivalent circuit is a combination of capacitor(s) and resistor(s). One commonly used equivalent circuit is the Randles circuit for fitting the impedance data.

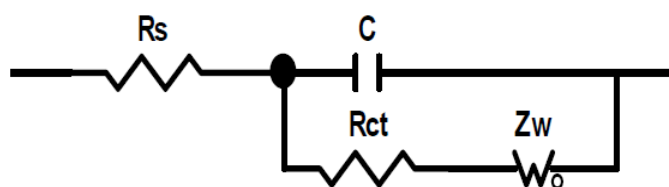


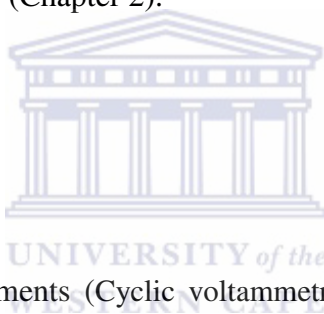
Figure 11. Randles equivalent circuit for simple electrochemical cell

From the circuit the above, electron transfer resistance (R_{ct}) at the electrode, and the capacitance, C , which is the ability of an electrochemical system to store or retain charge and Z_w is the Warburg impedance associated with the resistance as a result of the diffusion of ions across the electrode/electrolyte interface. Thus, EIS can give useful information of the impedance changes on the electrode surface before and after modification.

3.3 Reagents and instrumentation

3.3.1 Reagents

All chemicals used in this study were purchased from Sigma – Aldrich (Pty) Ltd., South Africa. The pyrrole (98%) was re-distilled at reduced pressure and saturated with argon atmosphere and stored in 1 mL ampoules in the dark at 4°C. Hydrochloric acid (32%) was used without further treatment. Deionised-distilled water used was prepared with Milli-Q water purification apparatus (Millipore). Antibody and Microcystin antigen congeners were obtained from the commercial Abraxis ADDA toxin kit. (Chapter 2).



3.3.2 Instrumentation

All voltammetric experiments (Cyclic voltammetry-CV, Osteryoung square wave voltammetry -OSWV and Differential Pulse voltammetry studies) were carried out with a BAS 100W automated electrochemical workstation (Bioanalytical Systems, Lafayette, IN, USA) room temperature. Electrochemical impedance spectroscopy (EIS) measurements were performed with a PGZ402 Voltalab Analyzer (Radiometer Analytical S.A, France). A conventional three-electrode cell was used. The electrodes were a glassy carbon disc electrode (GCE) with a surface area of 0.071 cm² as the working electrode (WE), a platinum wire auxiliary electrode (AE) and Ag/AgCl (3 M NaCl type; BAS MF-2052) reference electrode (RE).

The working electrode was cleaned by polishing, using circular motions, on slurries of 1.0 μm , 0.3 μm and 0.05 μm alumina powders (Bueller, IL, USA) placed on individual alumina pads, and rinsed with deionised water obtained by passing distilled water through a Milli-Q water purification apparatus (Millipore). Intermittently between usages, the electrodes were treated in hot concentrated H_2SO_4 and 30% H_2O_2 and washed with distilled deionised water. The counter electrode (AE) was cleaned between each experiment by heating in a Bunsen flame, washed and thoroughly rinsed with plenty of deionised water. The polypyrrole film was prepared from 35.ug/L of pyrrole, pre-treated by degassing with argon, added to a electrochemical cell containing 5 mL of degassed 0.1 M HCl (pH 7.0).



Chapter 4

Results and discussion

4.1 Instrumentation :

Electrochemical experiments were performed with a BAS 100W electrochemical workstation and electrodes from Bio-Analytical Systems, BAS, USA. Cyclic and square wave and differential pulse voltammograms were recorded with a computer interfaced to the BAS 100W workstation.

A glassy carbon disk electrode (GCE) with a surface area 0.071 cm^2 (diameter, 3mm) was used as the working electrode. A platinum wire and Ag/AgCl (3 M NaCl) electrodes were used as auxiliary and reference electrodes, respectively. The GCE was cleaned by polishing, using circular motions, on slurries of $1.0 \mu\text{m}$, $0.3 \mu\text{m}$ and $0.05 \mu\text{m}$ alumina powders (Bueller, IL, USA) placed on individual alumina pads, and rinsed with deionised water obtained by passing distilled water through a Milli-Q water purification apparatus (Millipore). The polished GCE was sonicated in millipore water after each consecutive polishing step. Polishing was done to ensure the removal any loosely-bound micro-particles. This pre-treatment process was also conducted to activate surface groups of the GCE for successful subsequent modification. All voltammetric results are reported with respect to Ag/AgCl reference electrode..

4.2 Synthesis of Polypyrrole

Pyrrole (98%) available from Sigma-Aldrich was distilled and placed into 1ml vials after being degassed with argon for 5 mins and stored in the dark at 4°C. Vials were degassed for 5 mins before being used in electrochemical experiments. Thin polypyrrole films were prepared from 0.1 M solutions of distilled pyrrole in an ionic solution of 0.1 M HCl (by adding 35.3 μ L of distilled pyrrole into 5 mL of 0.1 M HCl). The choice of 0.1M HCl was based on work done by Akinyeye *et al* [78] that showed that a clear and unambiguous potential window between -400 and 700 mV allowed for characterisation of peaks resulting from polypyrrole within the same potential window. The choice of an electrolyte concentration of 0.1 M HCl was based on the finding that higher concentration of 0.5 M and 1.0 M HCl causes undesirable and accelerated oxidation of the pyrrole monomer before application of potential [78].

To prevent over-oxidation of the polymer the electrolyte solution was purged by de-gassing with a gentle flow of argon gas for 15 min prior to usage and keeping the argon atmosphere on the electrolyte during polymerisation and characterisation processes. The films were grown potentiodynamically with a scan rate (v) of 50 mV/s by adding 35.3 μ L of Pyrrole to a glass electrochemical cell containing 5 mL of 0.1 M HCl. The electro-synthesised films were dried in air for about 5 min prior to characterisation in fresh 0.1 M hydrochloric acid solution. The cyclic voltammogram for the electropolymerization of undoped polypyrrole film on a GCE is shown in figure below. The electrochemically polymerized film, grown at a scan rate (v) of 50 mV/s for 10 cycles was observed to have good adhesion to the GCE surface.

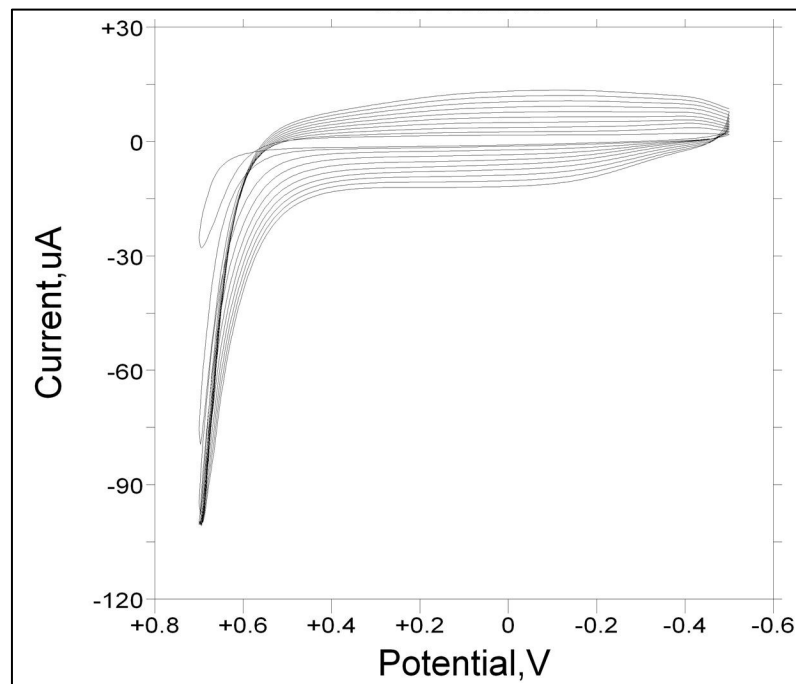


Figure 12. Cyclic Voltammogram of the polymerization of Polypyrrole in 0.1 M HCl over the potential window of -400 to 700 mV at a scan rate of 50 mV/s for 10 cycles on a GCE electrode.

The CV does not produce well defined oxidation and reduction peaks. The observation is in keeping with the findings of others[78]. This is due to the polymerization in a supporting electrolyte that has a small anionic dopant that could not produce an electroactive polymer with reversible or quasi-reversible electrochemistry. Larger dopant were investigated (ZrO_2^- ; WO_3^-) however of the dopants solubility was not easily achieved.

4.3 Characterization of Polypyrrole Modified Glassy Carbon electrode (GCE)

CV is very often used to characterize conducting polymer films. This is often the most favoured method for studying the reversibility of electron transfer because the oxidation and reduction can be monitored in the form of a current–potential diagram. Cyclic voltammetry results of polypyrrole-modified GCE electrode (GCE/PPY) is given below in the Figure 13.

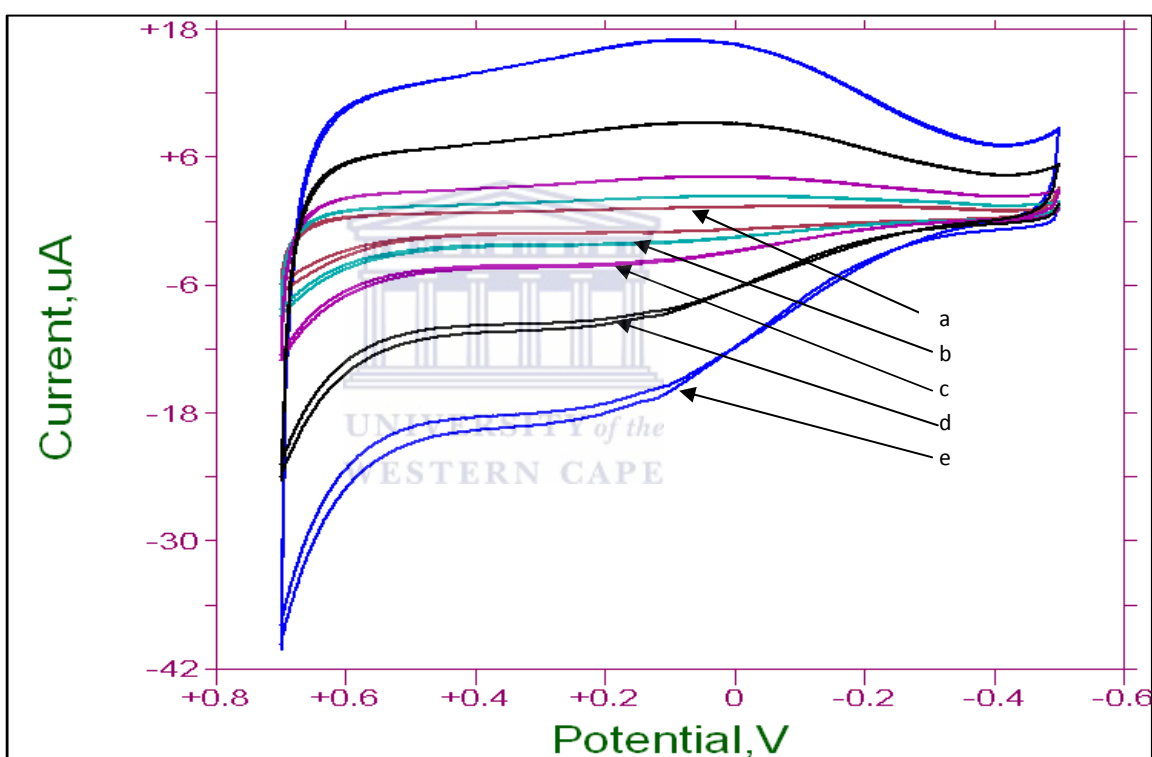


Figure 13. Characterization GCE/PPy electrode at different scan rates (a=5, b=10, c= 20, d= 50 & e= 100 mV/s) using cyclic voltammetry.

The GCE/PPy electrode was characterised in fresh 0.1 M HCl at a different scan rates. There was an observed increase in anodic and cathodic peak currents with increasing scan rates over the potential window -500 to 700 mV/s. Brown-Anson plots in figure 4.3 were drawn to determine the surface concentration of the

polymer films. Film thickness was not determined, thus the diffusion coefficients were calculated as a function of film thickness (L) using the Randle-Sevcik Equation.

$$D_e/L \text{ for undoped polypyrrole} = 3.36 \times 10^{-3} \text{ cm}^2/\text{s}$$

$$\text{Randle sevcik equation} \rightarrow \frac{I_{pa}}{v^{1/2}} = \frac{0.4463(nF)^{3/2} AD_e \Gamma^*}{L(RT)^{1/2}}$$

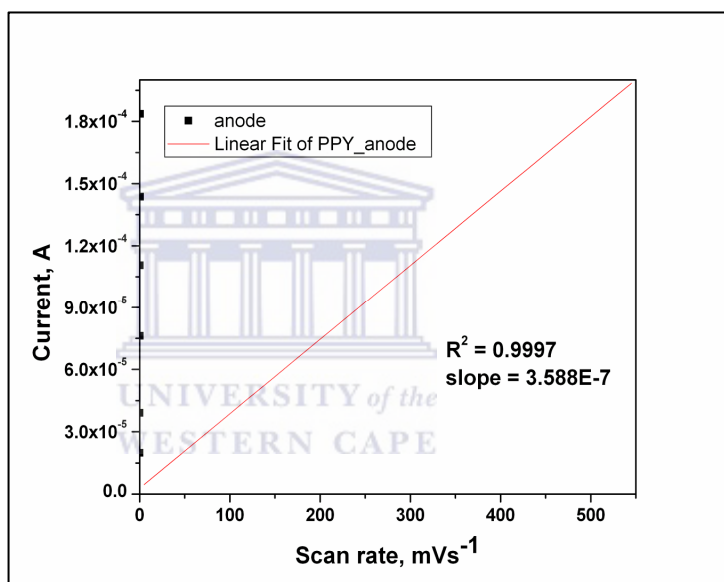


Figure 14. Plot of Square root of scan rate vs Current (A) for GCE/PPY film in 0.1 M HCl.

After characterization the electrodes were carefully cleaned. The CGE/PPY was thoroughly rinsed with millipore water and care was taken not to disturb the polypyrrole film on the electrode surface. The Ag/AgCl electrode was rinsed thoroughly and the reference electrode (Pt-wire) subjected to a Bunsen flame for 1 min to remove all impurities. A fresh Electrochemical cell was assembled with the supporting electrolyte made up of 7.0 pH , 0.1 M PBS. A few sweeps of cycle

voltammetry sweeps at 50 mV/S was done in the PBS to condition the polypyrrole-modified electrode. This served to condition the electrode and remove any residual acid (HCl analyte).

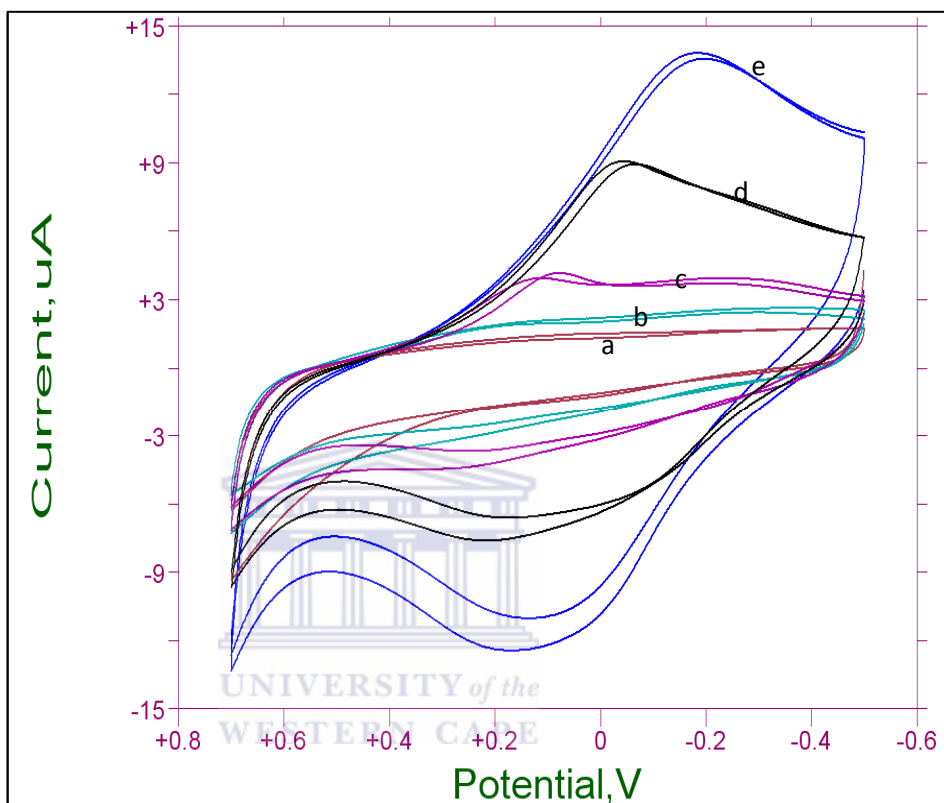


Figure 15. Characterization of GCE/PPY in 0.1 M PBS (pH 7.0) at scan rates (a=5, b=10, c= 20, d= 50 & e= 100 mV s)

The characterization graph for the polypyrrole modified glassy carbon electrode in 0.1 m PBS is depicted (figure 15). Anodic peaks and cathodic peaks show in increase and decrease peak heights respectively with increased scan rates.

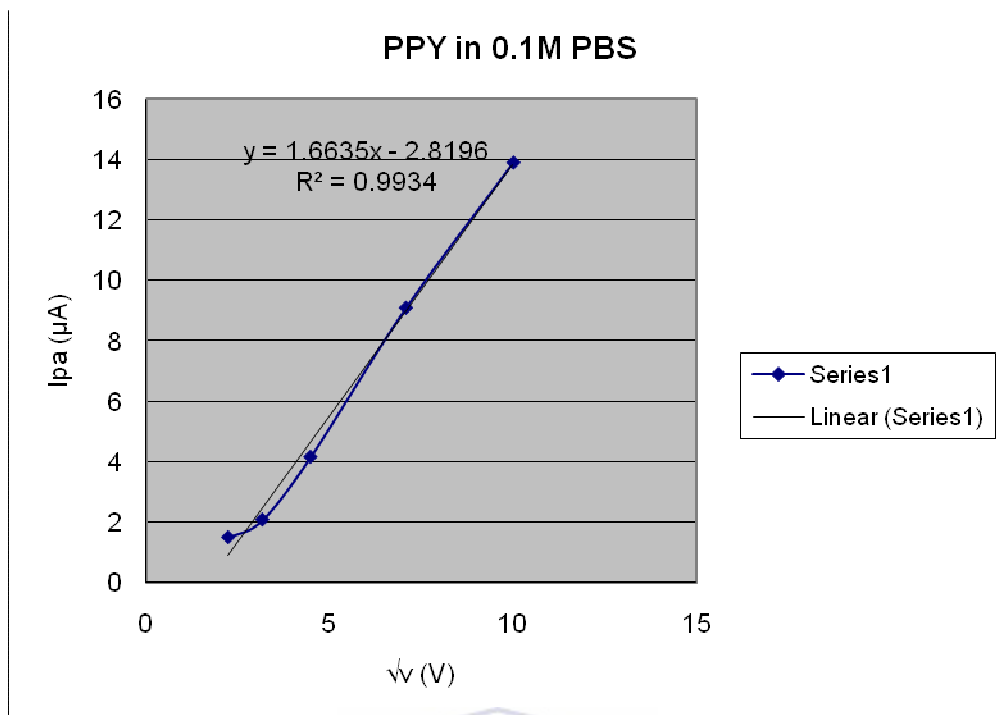


Figure 16. Plot of Square root of scan rate vs Current (I_{pa}) of for GC/PPY in PBS 0.1M PBS (pH7.0)

The D_e calculated on the trace generated at the 50mV/S in figure 14 was $8.79518 \times 10^{-8} \text{ cm}^2/\text{s}$

In both multi-scan rate voltammograms of the GCE/PPY electrode in 0.1 M HCl and 0.1M PBS (figure 13 and figure 15 respectively), both sets of peak potentials and corresponding peak currents varied, this possible indicates that the polymer was electroactive and diffusion of electrons was taking place along the polymer chain.

4.4 Preparation of Immunosensor

The polypyrrole-modified glassy carbon electrode (GCE/PPY) was air dried for 10 minutes after characterization steps described above. An accurate 10μl of Antibody solution (polyclonal anti-microcystins) was drop-coated onto the GCE/PPY surface and allowed to incubate overnight at 8°C for approximately 12-16 hours. The polyclonal antibody was obtained from a commercially available

ELISA kit produce by Abraxis and is a patented antibody raised in mice (Mouse IgG1). Following the initial incubation, a further 10 $\mu\text{g/L}$ of antibody solution was added to the GCE/PPY. The freshly formed immunosensor (GCE/PPY/AB) was covered with a lid and allowed to dry at room temperature for 1-2hrs. All further electrochemical experiments were carried out in 0.1 M PBS (pH 7.0) vs a Ag/AgCl reference electrode.

4.5 Cyclic Voltammetry.

4.5.1 Cyclic Voltammetric Investigation of Immunosensor

The prepared GCE/PPY/AB immunosensor was investigated with CV over a potential window of -500/700 mV, with increasing scan rates (10, 20, 50 and 100 $\text{mV}\cdot\text{s}^{-1}$) in 5mls of 0.1 M PBS (pH 7.0). No distinct peaks are observed at all of the scan rates. The electro-conductivity was observed to increase with increasing scan rates, however, there was no change in conductivity as observed in the voltamogramme trace for curves for 50 and 100 $\text{mV}\cdot\text{s}^{-1}$, (both yielded identical curves in figure 17 (c=d)). The formal potential could not be determined from the data CV (figure 17). More sensitive voltammetric methods (OSWV and DPV) were thus used to observe the immunosensor responses over a potential range

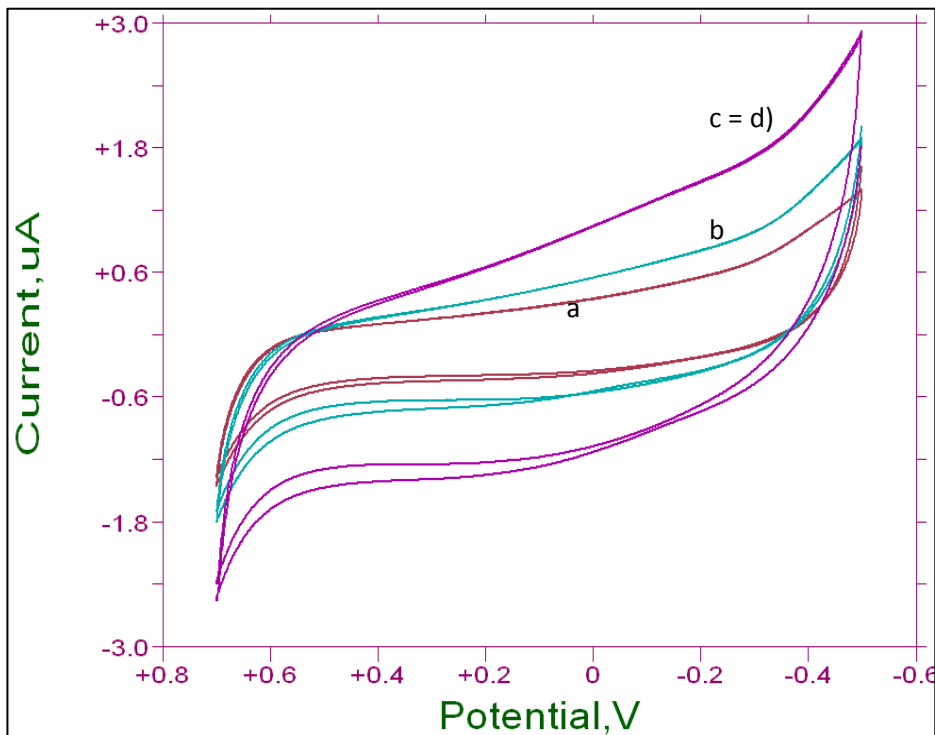


Figure 17. The multi –scan rate cyclic voltammograms for the Immunosensor (GCE/PPY/AB) (a= 10, b =20, c=50 and d = 100 mV/s)

4.5.2 Square Wave (OSWV) Voltammetric Investigation Of Immunosensor

The immunosensor ,GCE/PPY/AB, was thus investigated using the more sensitive method of OSWV. The Potential window for the forward oxidative sweep was started from the initial E of -500 mV to the final E of +700 mV.

Figure 18 and figure 19 shows the multi-scan rate using OSWV of the immunosensor (GCE/PPy/AB) for the Anodic and Cathodic sweeps.

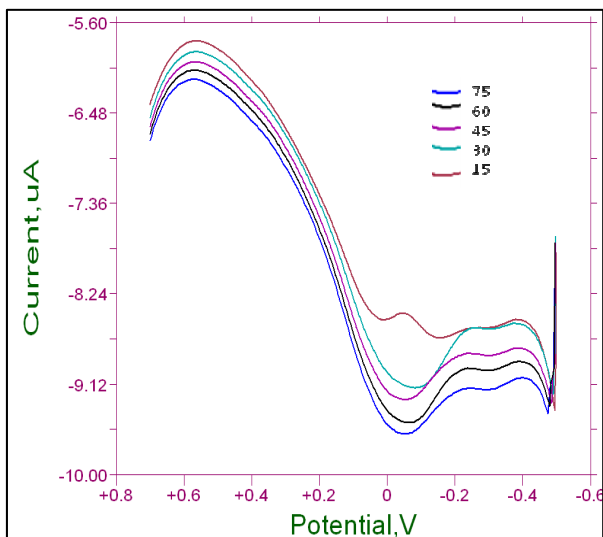


Figure 18. Multi-scan rate using OSWV of the immunosensor (GCE/PPy/AB) for the Anodic sweep

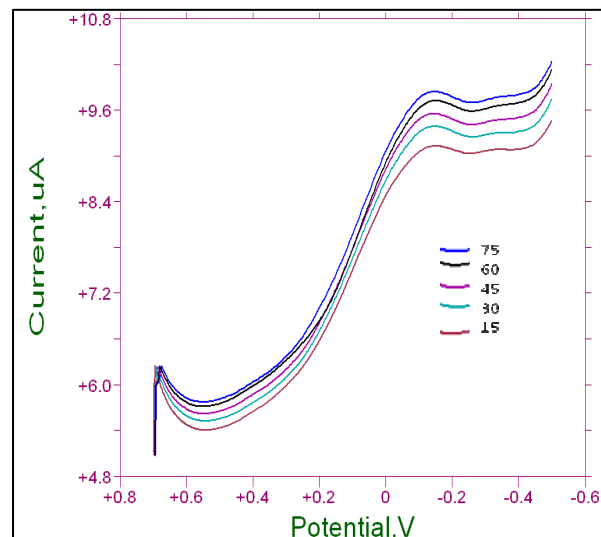


Figure 19. Multi-scan rate using OSWV of the immunosensor (GCE/PPy/AB) for the Cathodic sweep

The Peak potential in anodic graphs shows decrease in current with increase scan rates and the cathodic graphs show an increase in peak current with increase scan rates. The formal potential ΔE for the immunosensor system was calculated to be -112 mV vs Ag/AgCl using the equation

$$\Delta E = (E_{pa} + E_{pc}) / 2$$

The formal potential was calculated based on the average cathodic and anodic peak potential determined at different scan rates (Table 5 below)

OSWV	Anodic	Cathodic	Formal
Scan rate mV/s	E_{pa}	E_{pc}	E_o (mV)
15	-149.6	-149.6	-149.6
30	-75.3	-145.5	-110.4
45	-51.9	-145.4	-98.65
60	-62.5	-145.4	-103.95
75	-49.8	-143.4	-96.6
	average E_o		-112

Table5. Average peak potentials calculated for different scan rates for the anodic and cathodic observed

4.5.3 Differential Pulse Voltammetric Investigation Of Immunosensor

The GCE/PPY/AB was also investigated using the more sensitive method of DPV. The Potential window for the forward oxidative sweep was started from the initial E of -500mV to the final E of +700 mV.

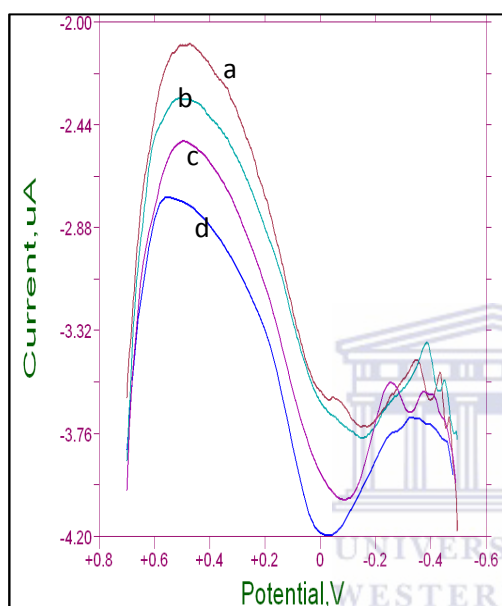


Figure 20. Multi-scan rate using DPV of the immunosensor (GCE/PPy/AB) for the anodic sweep*

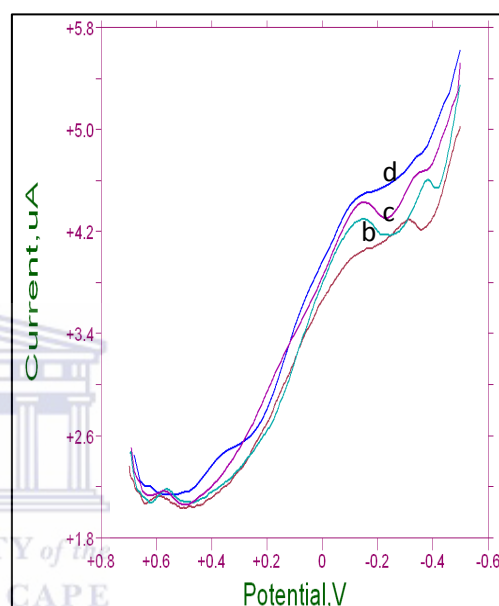


Figure 21. Multi-scan rate using DPV of the immunosensor (GCE/PPy/AB) for the cathodic sweep*

*Note: for both graphs a = 10, b -20 c = 5- and d = 100 mV/s

Figures 20 and 21 depict the multi-scan rate using DPV of the immunosensor (GCE/PPy/AB) for the anodic and cathodic sweep respectively. The formal potential for the immunosensor system was calculated to be -124 mV vs Ag/AgCl using the equation for ΔE ($\Delta E = (E_{pa} + E_{pc}) / 2$). The formal potential was calculated based on the average cathodic and anodic peak potential determined at different scan rates (Table 6)

DPV		Anodic	Cathodic	Formal
Scan rate mV/s		E _{pa}	E _{pc}	E _o (mV)
10		-158.1	-134.7	-146.4
20		-153.9	-145.4	-149.65
50		-85.9	-147.5	-116.7
100		-26.4	-141	-83.7
		average E _o		-124

Table 6. Average peak potentials calculated for different scan rates for the anodic and cathodic observed

The values for formal potential of the immunosensor system as determined by square wave voltammetry and differential pulse voltammetry are in good agreement. These formal potential was used in the evaluation of antigen binding to the immunosensor and for the calibration curve development and real sample analysis.



4.6 Development of Calibration curves

The immunosensor was calibrated by varying the addition of known amounts of antigen concentration. Since OSWV and DPV were the only two methods used, that were sensitive enough to observe changes in peak potentials at different scan rates, the development of the calibration curves were undertaken by these two methods. The Immunosensor GCE/PPy/AB was setup as the working electrode in a three as described previously using SWV and DPV techniques. Microcystin antigen standard, with a concentration of 1 μ g/l was added to the 5mL electrolyte 0.1M PBS solution (pH7.0). The antigen was added in aliquots of 2 μ l. After each

standard addition the OSWV and DPV traces were run at scan rates 60 mV/s and 50 mV/s respectively. The resultant anodic and cathodic curves are depicted in Figures 22(a) and 22(b).

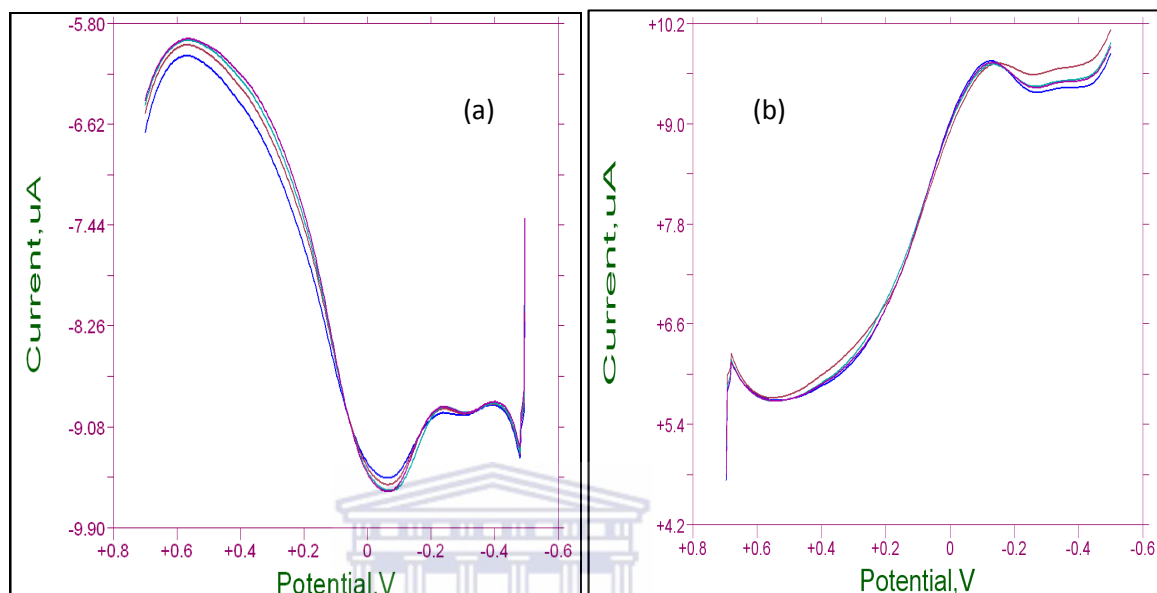


Figure 22. Oxidative (a) and reductive (b) OSWV for immunosensor response to increasing Antigen concentration.

The cathodic sweep did not reveal clear changes in cathodic peak current (I_{pc}). The data from this could not be used. Table 7 shows the concentrations and current differences used to construct the calibration curves for the Square wave Analysis (see Figure 24 and 25)

Table 7. Calibration curve data for OSWV

OSWV	OX	Difference	Concentration of Antigen	RED	Difference	Concentration of Antigen
	<i>i</i>	µA	µg/l	<i>i</i>	µA	µg/l
AB	-9.499E-06	0.000E+00	0	9.726E-06	0.000E+00	0
AG1	-9.552E-06	5.300E-08	3.998E-04	9.716E-06	1.000E-08	3.998E-04
AG2	-9.601E-06	1.020E-07	7.994E-04	9.733E-06	-7.000E-09	7.994E-04
AG3	-9.609E-06	1.100E-07	1.199E-03	9.756E-06	-3.000E-08	1.199E-03

The anodic sweep showed a clearer change in peak current response, with the addition of antigens, than the cathodic sweep. The changes in cathodic peak current (I_{pc}) was smaller in comparison to the Anodic peak responses. Table 8 shows the concentrations and current differences used to construct the calibration curves for the DPV Analysis (see Figure 26 & 27)

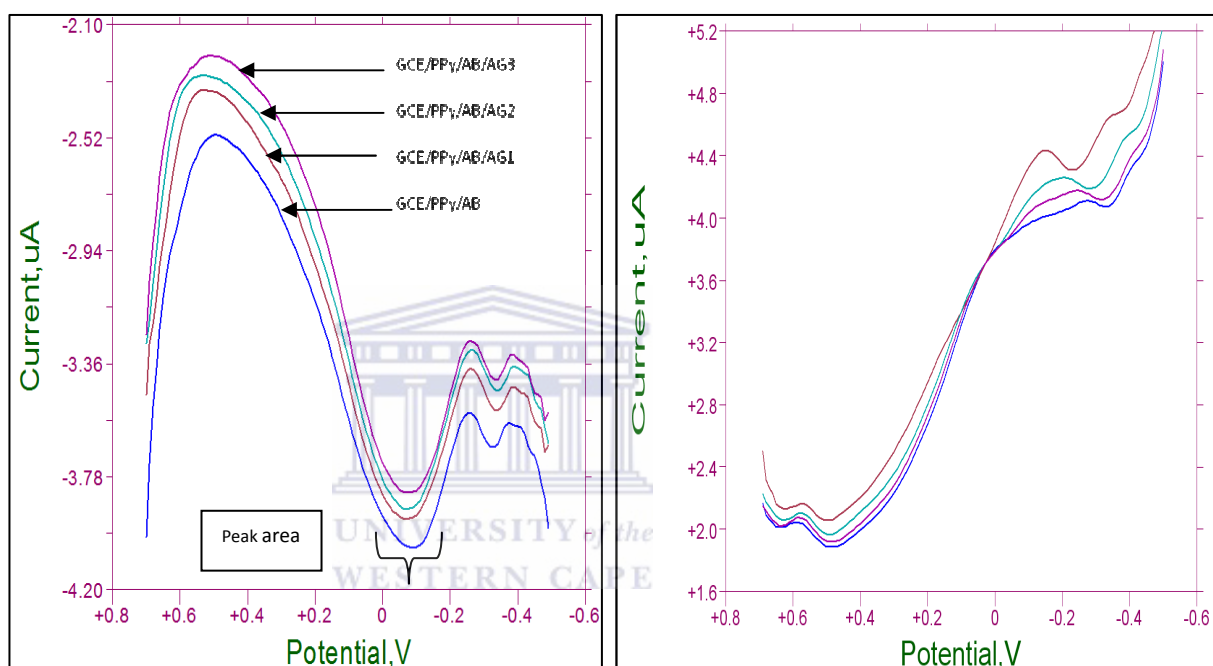


Figure 23. Oxidative (left) and reductive (Right) DPV for immunosensor response to increasing Antigen concentration and a scan rate of 50 mV/s

Table 8. Calibration curve data for DPV

DPV	OX	Difference	Concentration of Antigen	RED	Difference	Concentration of Antigen
	<i>i</i>	μA	$\mu\text{g/l}$	<i>i</i>	μA	$\mu\text{g/l}$
AB	-4.042E-06	0.000E+00	0	2.057E-06	0.000E+00	0
AG1	-3.935E-06	1.070E-07	3.998E-04	1.967E-06	9.000E-08	3.998E-04
AG2	-3.879E-06	1.630E-07	7.994E-04	1.916E-06	1.410E-07	7.994E-04
AG3	-3.834E-06	2.080E-07	1.199E-03	1.890E-06	1.670E-07	1.199E-03

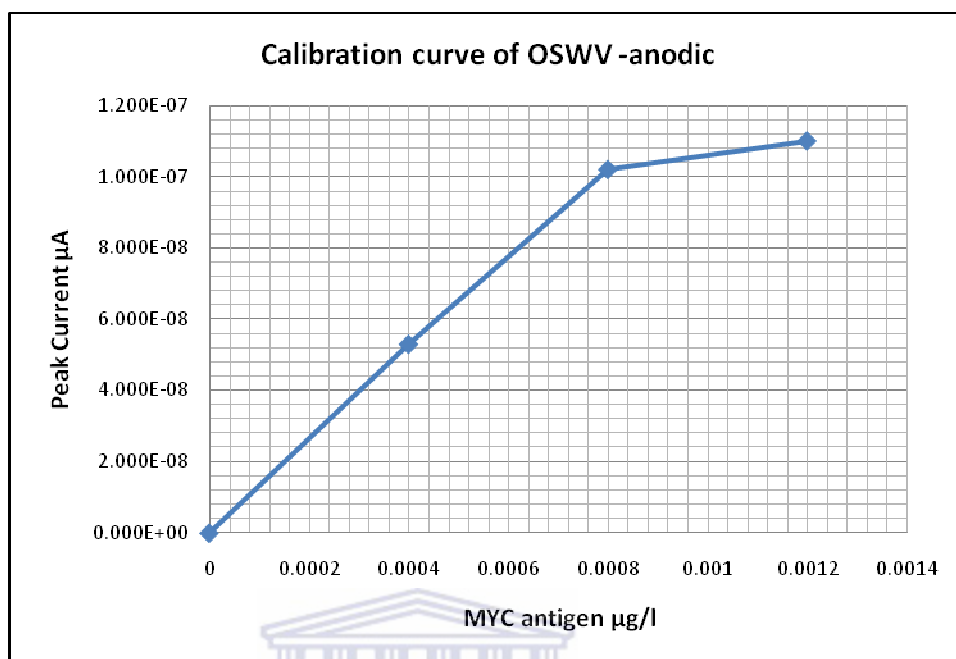


Figure 24. Calibration curve using anodic OSWV peak response.

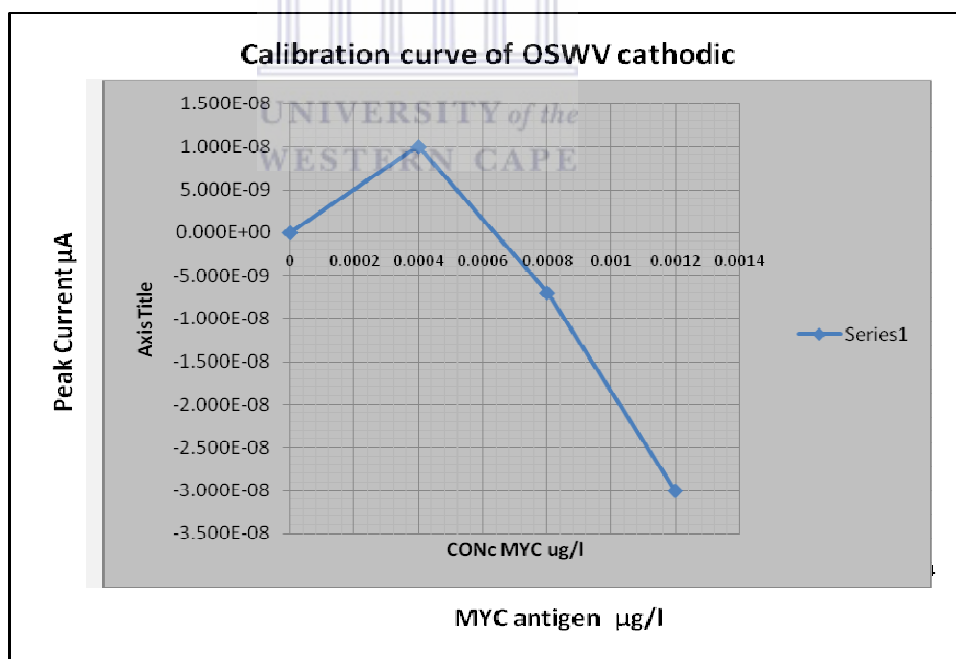


Figure 25. Calibration curve using cathodic SWV peak response

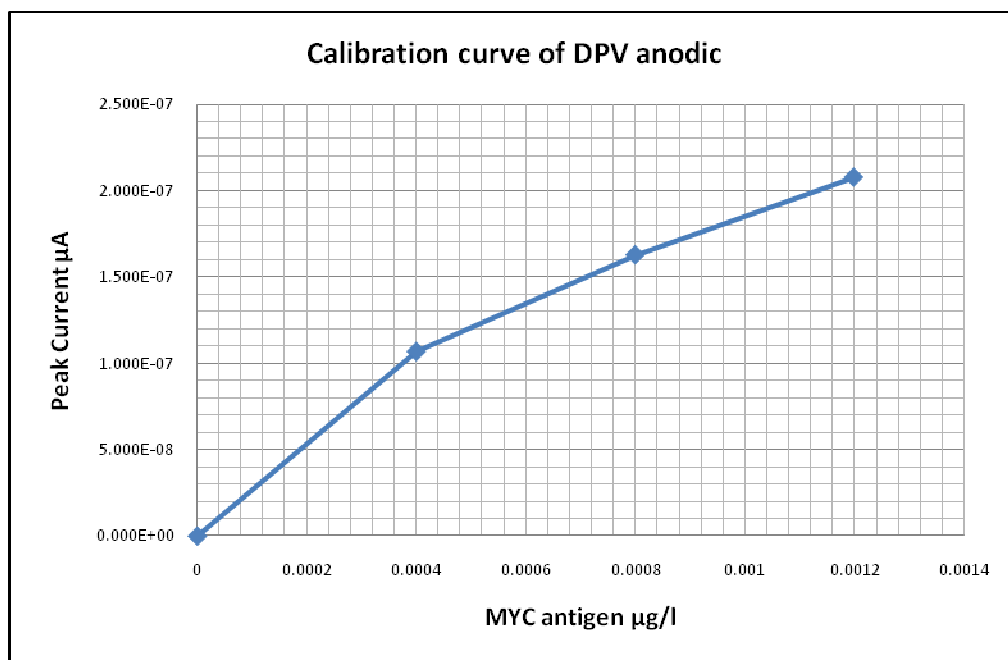


Figure 26. Calibration curve using anodic DPV peak response

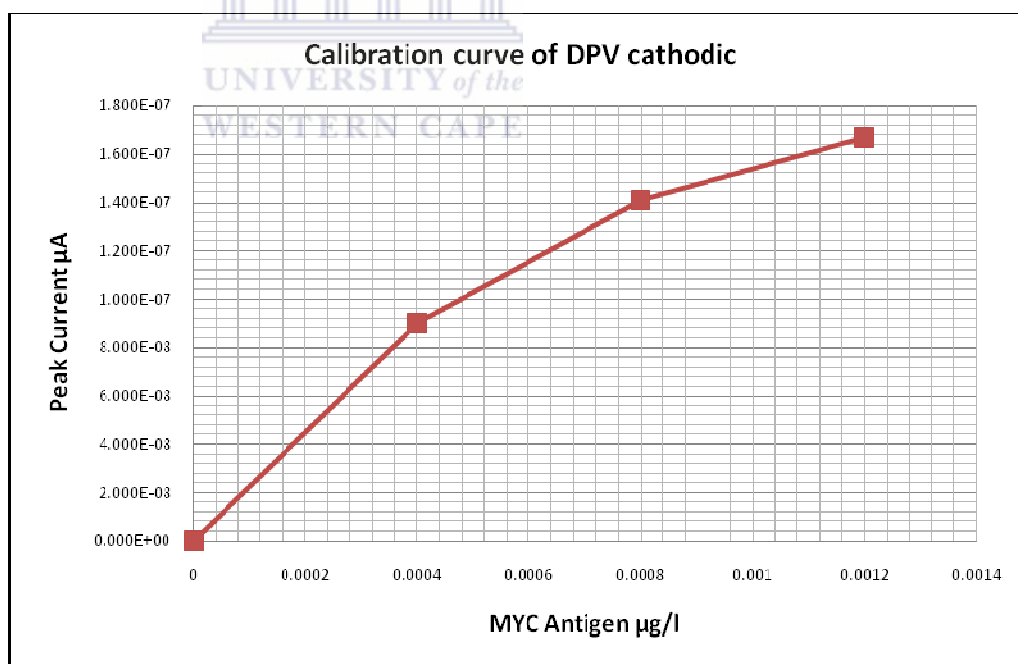


Figure 27. Calibration curve using cathodic DPV peak response

The anodic peak response showed the approach to saturation and hence levelling off of the XY plot, at the highest concentration of antigen added to solution (1.2×10^{-3}). The cathodic peak response to the Antigen-Antibody (Ag-Ab) binding event did not show the levelling off at the highest concentration detected indicating that the anodic current response was faster and is most likely the dominant catalytic mechanism for monitoring the Ab-Ag binding event. The same behaviour was observed using SWV and DPV current response. The calibration curve for the Cathodic OSWV results were inconclusive.

4.7 Real samples analysis:

The polypyrrole modified immunosensor was used to investigate the binding response of real samples taken from the raw dam waters intended for drinking water purposes. The samples analysed were from Voëlvlei Dam and pre-treated by sonication to release any microcystin antigens from the algae and to arrest any biological activity. Samples were then filtered with syringe filters ($0.45 \mu\text{m}$ pore size GFC Whatmann).

4.7.1 Differential Pulse Voltammetric Investigation Of Immunosensor and Real Samples

The antigen antibody binding events were observed in the sample matrix (figures

28 & 29

Figure 28. OSWV of immunosensor (GCE/PPY/AB) anodic response to real samples from Voëlvlei Dam

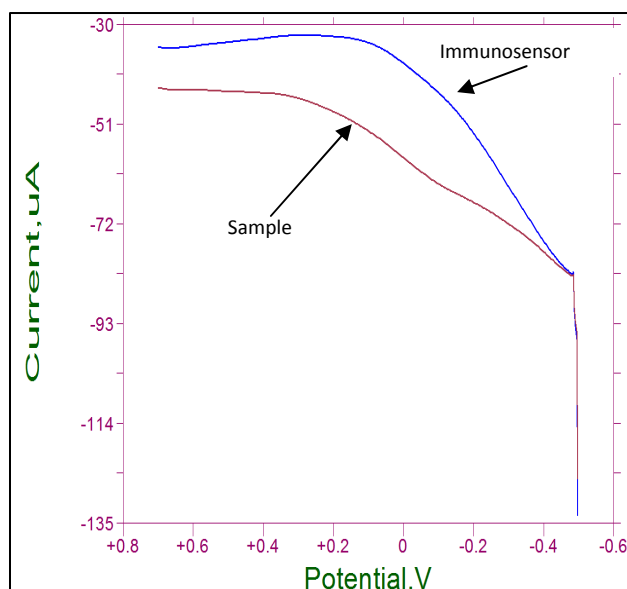
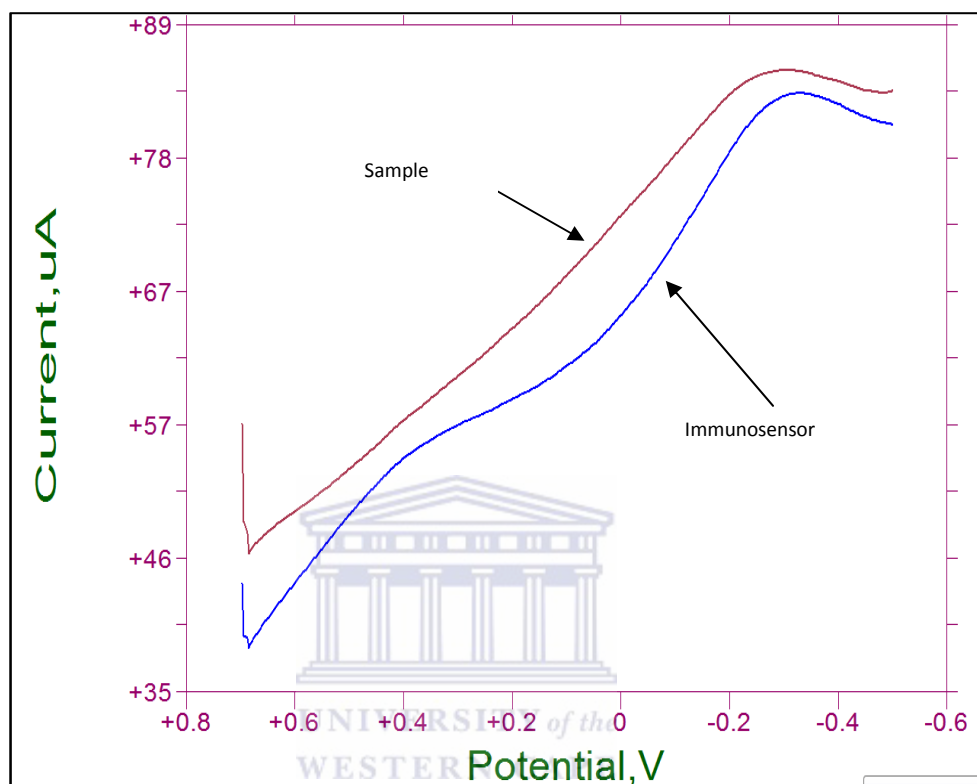


Figure 29. OSWV of immunosensor (GCE/PPY/AB) anodic response to real samples from Voëlvelei dam



The immune sensor does show a response to the antigen antibody binding at the electrode surface. Oxidative and reductive OSWV for immunosensor appears to have responded to an unknown concentration of antigens in the sample matrix.

The current difference of the oxidative peaks for sample response and baseline immunosensor taken at the calculated formal potentials of 104 is given in the

Table 9. The concentrations for the unknowns could be calculated.

Table 9. Table 4.5 : Showing the Peak currents and difference in peak currents of sample and immunosensor using OSWV

Voelvlei Dam Raw Water		current (μA)	Difference AB - (AB/SMP)(μA)
OSWV OX	AB	-4.490E-05	
	AB + SMP	-6.356E-05	1.866E-05
OSWV RED	AB	7.174E-05	
	AB + SMP	7.875E-05	-7.010E-06

AB= antibody; AB+SMP = antibody with sample.

4.7.2 Differential Pulse Voltammetric investigation of immunosensor and real sample

The antigen antibody binding events were observed in the sample matrix and showing Figures 30 (a) and (b)

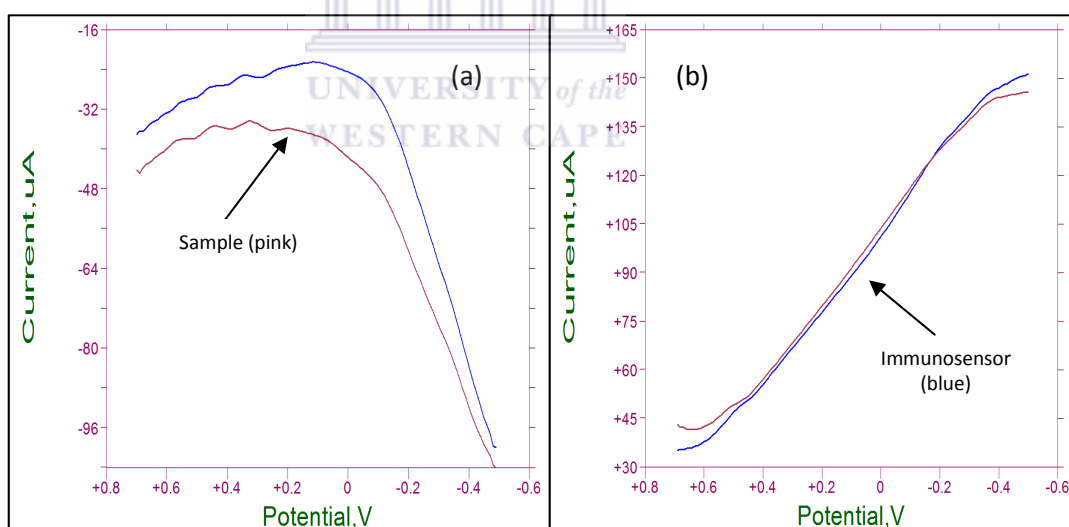


Figure 30. DPV of immunosensor (GCE/PPY/AB) anodic response (a) and cathodic response (b) to real samples from Voelvlei dam

Table 10. Showing the Peak currents and difference in peak currents of sample and immunosensor using DPV

Voëlvlei Dam Raw Water			
		current (μA)	Difference AB - (AB/SMP)(μA)
DPV OX	AB	-2.247E-05	
	AB + SMP	-3.706E-05	1.459E-05
DPV RED	AB	1.165E-04	
	AB + SMP	1.191E-05	1.046E-04

The decrease in current observed in the sample was related to the decrease in current as a result for the antibody-antigen binding and could be related to the concentration of the antigen in the sample using the calibration curves set up for DPV and SWV. It should be noted that the DPV was more sensitive on the anodic potential sweep. The cathodic curve could not be used.

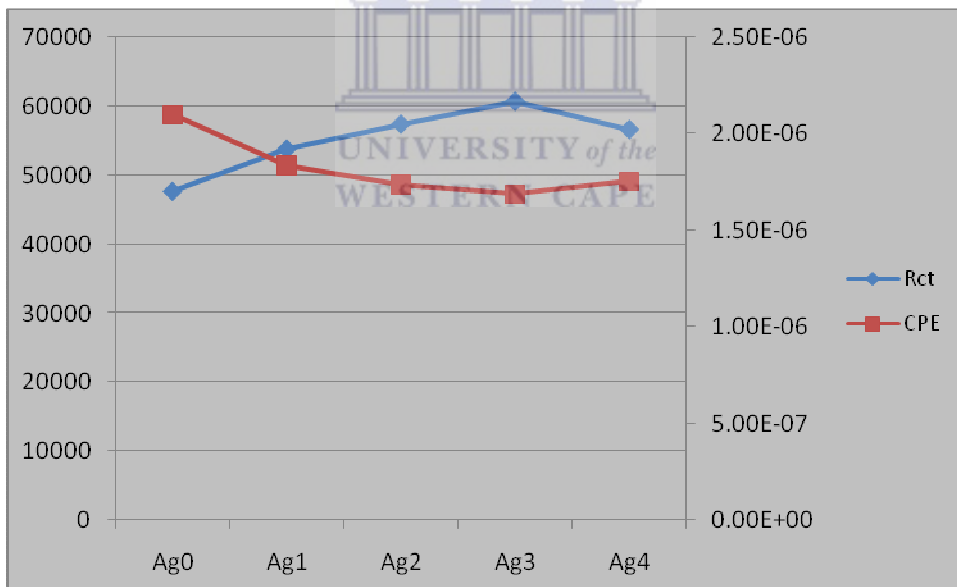
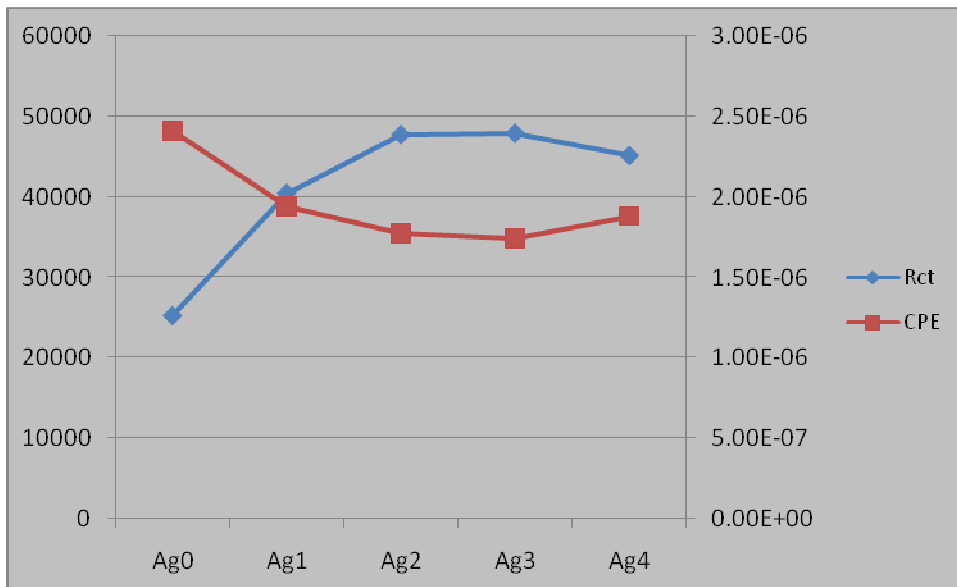
The real concentrations for the results were comparable to the results obtained by ELISA method. This was only true for the Anodic currents of DPV and OWSV.

ELISA results for Dam	0.28ug/l MYC	Method Acceptable error 10%
Immunosensor estimated result	0.14ug/l MYC	Error to be determined in future work

Table 11. Comparison of results from ELISA and Immunosensor

NB. Immunosensor result was diluted during the investigation.

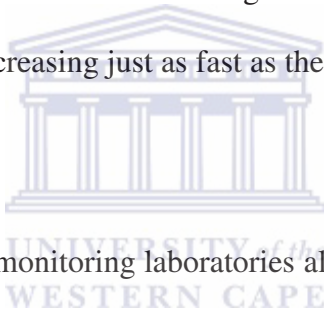
4.8 Electrochemical Impedance Spectroscopy (EIS) results



Chapter 5:

Conclusions

The monitoring of cyanotoxins continues to be a major concern facing modern society. The detection of cyanotoxins and in particular MCN's has gone through number improvements. The emphasis on increase sensitivity and the ability detect lower concentrations has been focus of many studies[39]. The analytical methods used for MCN's and specifically for Microcystin –LR can be divided into those that are used as screens i.e. they detect the presence of toxins and generally don't need pre-treatment of samples, and those that are used for the identification and quantification of various individual toxins and require elaborate and tedious pre-treatment and concentration steps. The Elisa Method is currently the method of choice in routine monitoring laboratories. However the costs of Elisa consumables are increasing just as fast as the demand for toxin testing.

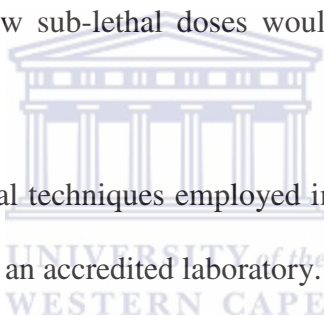


Accreditation of routine monitoring laboratories also places extra pressure on labs to perform the lab analysis to a strictly controlled set of criteria. The need for accreditation is necessary to maintain a global standard of general laboratory practice that can sustain results that are reputable. The need for an accredited toxin analysis that is both cost effective and accurate and can conform to the demands of an accredited laboratory is being sought. Biosensors are fast becoming the methods of choice for routine monitoring laboratories. Biosensor applications are varied owing to the easy assembly and low production costs effective.

This work showed that the polypyrrole-modified immunosensor was responsive to the presence of microcystin toxin in real samples, based on the antibody antigen binding reaction specificity. While there is lots of refining needed in the production of the immunosensor, the principle of antigen-antibody binding reaction can be investigated further by electrochemical analysis techniques.

The Immunosensor was sensitive to lower dosages of toxin when compared to the ELISA method. It is predicted that future work would show that the immunosensor would be sensitive to lower concentrations below the detection limit of the ELISA methods. This would be beneficial to the routine monitoring of algal toxins since the low sub-lethal doses would be detected early during the water treatment process.

Furthermore the analytical techniques employed in electrochemistry would easily conform to the rigours of an accredited laboratory.



References

1. Sonjica B. , M.o.W.a.E.A. *Welcome note to 2nd Africa Water Week*. [Web Page] 2009 [cited 2009; Available from: http://www.dwaf.gov.za/dir_ws/2aww/Buyelwa_Patience_Sonjica.asp].

2. Nyenje, P.M., et al., *Eutrophication and nutrient release in urban areas of sub-Saharan Africa -- A review*. Science of The Total Environment, 2010. **408**(3): p. 447-455.
3. Mogakabe, E. *National Eutrophication Monitoring Programme*. 2009 [cited 2011; Available from: <http://www.dwa.gov.za/iwqs/eutrophication/NEMP/>].
4. Li, X.-Y., et al., *Toxicity of microcystins in the isolated hepatocytes of common carp (Cyprinus carpio L.)*. Ecotoxicology and Environmental Safety, 2007. **67**(3): p. 447-451.
5. Zhu, W., L. Wan, and L. Zhao, *Effect of nutrient level on phytoplankton community structure in different water bodies*. Journal of Environmental Sciences, 2010. **22**(1): p. 32-39.
6. Van Ginkel, C.E., *A national Survey of incidence of cyanobacterial blooms and toxins productions in major impoundments.*, in *National Eutrophication Monitoring Programme*. 2003: Pretoriz.
7. Harding, W.R., et al., *An overview of cyanobacterial research and management in South Africa post-2000*. Water SA, 2009. **35**(4): p. 479-484.
8. de Figueiredo, D.R., et al., *Microcystin-producing blooms--a serious global public health issue*. Ecotoxicology and Environmental Safety, 2004. **59**(2): p. 151-163.
9. Chorus, I.B.J.e., *Toxic Cyanobacteria in Water: A guide to their public health consequences, monitoring and management*. First ed, ed. C.I.B. J. 1999, Geneva: WHO.
10. Yoo, R., Carmichael, W., Hoehn, R. and Hrudley, S., *Cyanobacterail (Blue-Green Algae) Toxins: A resource Guide*. 1995, American Water Works Association Research Foundation: Denver.
11. Rositano, J.G.N., B. Nicholson and P. Sztajnbok, *The effect of Water Quality on the Destruction of Cyanotoxins*, in WISA, J. Rotisino, Editor. 2000: Sun City South Africa.
12. Zohary T. , M.A., *Structural, physical and chemical charactersitics of Microcystis aeroginosa hyperscums from a hypertrophic lake*. Freshwater Biology, 1990. **23**: p. 339-409.
13. Ned Butler, J.C.C., Regina Linville, Barbara Washburn, *Microcystins : A brief overview of their toxicity and effects, with special reference to fish, wildlife, and livestock*. 2009, Department of Water Resources, Resources gency.
14. Msagati, T.A.M., B.A. Siame, and D.D. Shushu, *Evaluation of methods for the isolation, detection and quantification of cyanobacterial hepatotoxins*. Aquatic Toxicology, 2006. **78**(4): p. 382-397.
15. Lahti, K., et al., *Persistence of cyanobacterial hepatotoxin, microcystin-LR in particulate material and dissolved in lake water*. Water Research, 1997. **31**(5): p. 1005-1012.
16. Azevedo, S.M.F.O., et al., *Human intoxication by microcystins during renal dialysis treatment in Caruaru--Brazil*. Toxicology, 2002. **181-182**: p. 441-446.
17. Baganz, D., G. Staaks, and C. Steinberg, *Impact of the cyanobacteria toxin, microcystin-lr on behaviour of zebrafish, danio rerio*. Water Research, 1998. **32**(3): p. 948-952.
18. Dietrich, D. and S. Hoeger, *Guidance values for microcystins in water and cyanobacterial supplement products (blue-green algal supplements): a reasonable or misguided approach?* Toxicology and Applied Pharmacology, 2005. **203**(3): p. 273-289.
19. Falconer, I., *Is there a Human Health Hazard from Microcystins in the Drinking Water Supply?* Acta hydrochim. hydrobiol, 2005. **33**(1): p. 64-71.

20. Botes, D.e.a., *Configuration assignments of amino acid residues and the presence N-methyldehydroalanine is toxins from the blue-green alga, Microcystis aeruginosa*. *Toxicon*, 1982. **20**: p. 1037-1042.
21. Fischer, W.D., D.R., *Toxicity of the cyanobacterial cyclic heptapeptide toxins microcystin-LR and -RR in early life-stages of the African claw frog (Xenopus laevis)*. *Aquatic Toxicology*, 2000. **49**: p. 189-198.
22. WHO, *Cyanobacterial toxins: Microcystin-LR in drinking-water. Background document for preparation of WHO Guidelines for drinking-water quality*. 2003, World Health Organization: Geneva.
23. Haddix, P.L., C. J. Hughley and M. W. LeChevallier., *Occurrence of microcystins in 33 US water supplies*. *Journal of the American Water Works Association*, 2007. **99**: p. 118-125.
24. Wang, M., et al., *Protein profiles in zebrafish (Danio rerio) brains exposed to chronic microcystin-LR*. *Chemosphere*, 2010. **81**(6): p. 716-724.
25. Milutinovic, A., et al., *Nephrotoxic effects of chronic administration of microcystins -LR and -YR*. *Toxicon*, 2003. **42**(3): p. 281-288.
26. Butler Ned, J.C.C., Regina Linville, Barbara Washburn, *Microcystins : A brief overview of their toxicity and effects, with special reference to fish, wildlife, and livestock*. 2009, Department of Water Resources, Resources gency.
27. Cardozo, K.H.M., et al., *Metabolites from algae with economical impact*. *Comparative Biochemistry and Physiology Part C: Toxicology & Pharmacology*, 2007. **146**(1-2): p. 60-78.
28. Yokoyama Atsushi, H.-D.P. (2003) *Depuration Kinetics and Persistence of the Cyanobacterial Toxin Microcystin-LR in the Freshwater Bivalve Unio douglasiae*. Published online in Wiley InterScience (www.interscience.wiley.com).
29. Oberholster, P.J., et al., *Identification of toxigenic Microcystis strains after incidents of wild animal mortalities in the Kruger National Park, South Africa*. *Ecotoxicology and Environmental Safety*, 2009. **72**(4): p. 1177-1182.
30. Freitas de Magalhães, V., R. Moraes Soares, and S.M.F.O. Azevedo, *Microcystin contamination in fish from the Jacarepaguá Lagoon (Rio de Janeiro, Brazil): ecological implication and human health risk*. *Toxicon*, 2001. **39**(7): p. 1077-1085.
31. Charles P. Debloisa, R.A.-R., Alessandra Gianic, David F. Birda, *Microcystin accumulation in liver and muscle of tilapia in two large Brazilian hydroelectric reservoirs*. *Toxicon*, 2008. **51**: p. 435-448.
32. Codd, G.A., J.S. Metcalf, and K.A. Beattie, *Retention of Microcystis aeruginosa and microcystin by salad lettuce (Lactuca sativa) after spray irrigation with water containing cyanobacteria*. *Toxicon*, 1999. **37**(8): p. 1181-1185.
33. Schaeffer, D.J., P.B. Malpas, and L.L. Barton, *Risk Assessment of Microcystin in Dietary Aphanizomenon flos-aquae*. *Ecotoxicology and Environmental Safety*, 1999. **44**(1): p. 73-80.
34. Hoeger, S.J., B.C. Hitzfeld, and D.R. Dietrich, *Occurrence and elimination of cyanobacterial toxins in drinking water treatment plants*. *Toxicology and Applied Pharmacology*, 2005. **203**(3): p. 231-242.
35. Yuan, M., W.W. Carmichael, and E.D. Hilborn, *Microcystin analysis in human sera and liver from human fatalities in Caruaru, Brazil 1996*. *Toxicon*, 2006. **48**(6): p. 627-640.
36. Suput, D. and B. Sedmak, *Hepatic dysfunction after acute and chronic exposure to microcystins*. *Pathophysiology*, 1998. **5**(Supplement 1): p. 102-102.

37. Batista, T., et al., *Microcystin-LR causes the collapse of actin filaments in primary human hepatocytes*. *Aquatic Toxicology*, 2003. **65**(1): p. 85-91.
38. Hernández, J.M., V. López-Rodas, and E. Costas, *Microcystins from tap water could be a risk factor for liver and colorectal cancer: A risk intensified by global change*. *Medical Hypotheses*, 2009. **72**(5): p. 539-540.
39. McElhiney, J. and L.A. Lawton, *Detection of the cyanobacterial hepatotoxins microcystins*. *Toxicology and Applied Pharmacology*, 2005. **203**(3): p. 219-230.
40. Kiviranta J, S.K., Niemela Sl., *Detection and toxicity of cynaobacteria by Artemia salina bioassay*. *Environ. Toxicol. Water Qual.*, 1991. **6**: p. 423-426.
41. Marsalek B. & Blaha L, *Comparison of 17 biotests for detection of cyanobacterial toxicity*. *Environmental Toxicology* 2004. **19**: p. 310-317.
42. Tarczynska M., N.-J.G., Romanowska-Duda Z., Sawicki J., Beattie K., Codd G. & Zalewski M., *Tests for the toxicity assessment of cyanobacterial bloom samples*. *Environmental Toxicology*, 2001 **16**: p. 383-390.
43. Kos P, G.G., Suranyi G. & Borbely G. , *Simple and Efficient Method for Isolation and Measurement of Cyanobacterial Hepatotoxins by Plant Tests (Sinapis alba L.)*. *Analytical Biochemistry* 1995. **225**: p. 49-53.
44. Romanowska-Duda Z, T.M., *Influence of microcystin-LR and hepatotoxic cyanobacterial extract on the water plant Spirodela oligorrhiza*. *Environmental Toxicology*, 2002. **17**(434 -440).
45. Gehringer M.M., K.V., Coates N. & Downing T.G. , *The use of Lepidium sativum in a plant bioassay system for the detection of microcystin-LR*. *Toxicon* 2003. **41**: p. 871-876.
46. Fastner J., H.R.C.I., *Microcystin-content, hepatotoxicity and cytotoxicity of cyanobacteria in some German water bodies*. *Water Science and Technology* 1995. **32**: p. 165-170.
47. Rapala, J., et al., *Detection of microcystins with protein phosphatase inhibition assay, high-performance liquid chromatography-UV detection and enzyme-linked immunosorbent assay: Comparison of methods*. *Analytica Chimica Acta*, 2002. **466**(2): p. 213-231.
48. Lawrence JF. et al *Cpmparison of Liquid Chromtography / Mass Spectrometry, ELISA, and Phosphatase Assay for the Determination of Microcystins in Blue-Green Algal Products*. *Journal of AOAC International*, 2001. **84**(4): p. 1035 - 1044.
49. Han, J., et al., *Highly sensitive detection of the hepatotoxin microcystin-LR by surface modification and bio-nanotechnology*. *Colloids and Surfaces A: Physicochemical and Engineering Aspects*. **In Press, Corrected Proof**.
50. Sangolkar . LN, M.S., Chakrabarti T, *Methods for determining microcystins (peptide hepatotoxins) and microcystin-producing cyanobacteria*. *Water Research*, 2006. **40**: p. 3485-3496.
51. Ueno, Y. and S. Nagata, *ELISA analysis of microcystins, algal hepatotoxins, in environmental water*. *Toxicon*, 1997. **35**(4): p. 482-483.
52. Metcalf J.S , S.G.B.a.G.A.C., *Production of Novel Polyclonal Antibodies against the Cyanobacterial Toxin Microcystin-LR and their application for the detection and quatification of Microcystins and Nodularins*. *Water Research*, 2000. **34**(10): p. 2761 - 2769.
53. Baiera W , M.L., B. Fischera, G. Jungc, U. Neumannb, M. Weiûa, J. Weckesserb, P. Hoÿmanna, W.G. Bessler a, K. Mittenbuÿ hler, *Generation of antibodies*

- directed against the low-immunogenic peptide-toxins microcystin-LR/RR and nodularin. *International Journal of Immunopharmacology* 2000. **22**: p. 339±353.
54. Fischer, W.e.a., *Congener-Independant Immunoassay for Microcystins and Nodularins*. *Environmental Science & Technology*, 2001. **35**: p. 4849-4856.
 55. Hawkins Peter R, S.N., Peter Cox, Brett A. Neilan, Brendan P. Burns, Glen Shaw, Wasa Wickramasinghe, Yuwadee Peerapornpisal, Werawan Ruangyuttikarn, Tomoaki Itayama, Takeshi Saitou, Motoyuki Mizuochi and Yuhei Inamori, *A review of analytical methods for assessing the public health risk from microcystin in the aquatic environment*. *Journal of Water Supply: Research and Technology—AQUA* 2005. **54**(8): p. 509-518.
 56. Robinson NA, P.J., Matson CF, Miura GA, Lawrence WB., *Tissue distribution, excretion and hepatic biotransformation of MCLR in mice*. *J. Pharmacol. Exp. Ther.*, 1991. **256** (1): p. 176–182.
 57. Peng, L., et al., *Health risks associated with consumption of microcystin-contaminated fish and shellfish in three Chinese lakes: Significance for freshwater aquacultures*. *Ecotoxicology and Environmental Safety*, 2010. **73**(7): p. 1804-1811.
 58. Ibelings, B.W. and I. Chorus, *Accumulation of cyanobacterial toxins in freshwater "seafood" and its consequences for public health: A review*. *Environmental Pollution*, 2007. **150**(1): p. 177-192.
 59. Ueno Yoshio, S.N., Tomoaki Tsutsumi, Akihiro Hasegawa, Mariyo F. Watanabe, Ho-Dong Park, Gong-Chao Chen, Gang Chen and Shun-Zhang Yus, *Detection of microcystins, a blue-green algal hepatotoxin, in drinking water sampled in Haimen and Fusui, endemic areas of primary liver cancer in China, by highly sensitive immunoassay*. *Carcinogenesis* 1996. **17**(6): p. 1317-1321.
 60. Shan Guomin, C.L., Shirley J. Gee and Bruce D. Hammock, *Immunoassay, biosensors and other nonchromatographic methods*, in *Handbook of Residue Analytical Methods for Agrochemicals*, P.W. Lee, Editor. 2002, John Wiley & Sons, Ltd, Chichester,.
 61. Biosense. *Measuring Principles of ELISA* <http://www.biosense.com/>.
 62. Zheng Michael Z., J.L.R.J.B., *A review of rapid methods for the analysis of mycotoxins*. *Mycopathologia* 2006. **161**: p. 261–273.
 63. Crowther, J.R., *The ELISA Guidebook*. *METHODS IN MOLECULAR BIOLOGY*, ed. John M. Walker. 2002, Totowa, New Jersey 07512: 2001 Humana Press Inc.
 64. James Ryan, A.G., and Amy Dindal, Battelle and U.S.E. John McKernan, *Abraxis Microcystin test kits: ADDA ELISA Test Kit, DM ELISA Test Kit, Strip Test Kit*, in *Environmental Technology Verification Report*, Battelle, Editor. 2010, ETV Advanced Monitoring Systems Center.
 65. Headquarters, B.U.S.-W. *Gen5 Data Analysis Software*. 2011; Available from: http://www.biotek.com/products/microplate_software/gen5_data_analysis_software.html.
 66. Zhou L , Y.H., Chen K, *Relationship between microcystin in drinking water and colorectal cancer*. *Biomedical & Environmental Sciences*, 2002. **15**: p. 166-171.
 67. Pyo D., H.Y., Kim Y. & Hahn J.H., *Ultra-sensitive analysis of microcystin-LR using microchip based detection system*. *Bulletin of the Korean Chemical Society*, 2005a. **26**: p. 939-942.
 68. Kim Y . S.W. Oh, S.Y.J., D.J. Pyo and E.Y. Choi, *Development of an ultrarapid one-step fluorescence immunochromatographic assay system for the quantification of microcystins* *Environ. Sci. Technol*, 2003. **37** p. pp. 1899–1904.

69. Campas M, M.J.-L., *Highly sensitive amperometric immunosensors for microcystin detection in algae*. *Biosensors and Bioelectronics*, 2007. **15**(22(6)): p. 1034-40.
70. Chianella I, M.L., S.A. Piletsky, I.E. Tothill, B. Chen, K. Karim and A.P.F. Turner, *Rational Design of a polymer specific for microcystin-LR using a computational approach*. *Anal. Chem.*, , 2002. **74** p. pp. 1288–1293. .
71. Chianella I , S.A.P., I.E. Tothill, B. Chen and A.P.F. Turner,, *MIP-based solid phase extraction cartridges combined with MIP-based sensors for the detection of microcystin-LR*. *Biosens. Bioelectron.*, , 2003. **18** p. pp. 119–127.
72. Osten D.E., J.M.P.J.K., *Surface plasmon resonance coupled with molecularly imprinted polymers for detecting microcystin-LR*. *Abstracts of Papers of the American Chemical Society*, 2005. **230**:: p. U1597-U1597.
73. **Bard, A.F., LR**, ed. *Electrochemical Methods - Fundamentals and Applications*. 2nd edition ed. 2001, John Wiley & Sons Inc.
74. Monk, P., ed. *Fundamentals Of Electroanalytical Chemistry*. 2001, John Wiley & Sons.
75. Kissinger P, H.W., *Cyclic voltammetry*. *Journal of Chemical Education*, 1983. **60**(9): p. 702.
76. Kounaves SP. *Voltammetric Techniques: Chapter 37, Handbook of Instrumental Techniques for Analytical Chemistry*.: 709-725 2007; Available from: <http://www.prenhall.com/settle/chapters/ch37.pdf>.
77. Manohar, A.K.O.B., Kenneth H. Neelson , Florian Mansfeld *The use of electrochemical impedance spectroscopy (EIS) in the evaluation of the electrochemical properties of a microbial fuel cell*. *Bioelectrochemistry* 2008. **72** p. 149–154.
78. Akinyeye RO, M.M., Sekota M, A hmed A-ALI, Baker P. & Iwuoha E., *Electrochemical Interrogation and Sensor Application of Nanostructured Polypyrroles*. *Electroanalysis*, 2006. **18**(24): p. 2441-2450.
79. Brett, C.M.A.B., A.M.O., *Electrochemistry Principles, Methods and Applications*. *Oxford University Press, United States, New York*. 2005.
80. Kang, X.M., Zhibin Zou, Xiaoyong Cai, Peixiang Mo, Jinyuan,, *A novel glucose biosensor based on immobilization of glucose oxidase in chitosan on a glassy carbon electrode modified with gold-platinum alloy nanoparticles/multiwall carbon nanotubes*. *Analytical Biochemistry*, 2007. **369**(1): p. 71-79.
81. Fernández-Sánchez, C., McNeil, C.J. & Rawson, K., , *Electrochemical impedance spectroscopy studies of polymer degradation: application to biosensor development*. . *Trends in Analytical Chemistry*, 2005. **24**(1): p. 37-48.